8-2004

Bit Loading and Peak Average Power Reduction Techniques for Adaptive Orthogonal Frequency Division Multiplexing Systems

Jaideep Rajan Shahri
University of Tennessee - Knoxville

To the Graduate Council:

I am submitting herewith a thesis written by Jaideep Rajan Shahri entitled "Bit Loading and Peak Average Power Reduction Techniques for Adaptive Orthogonal Frequency Division Multiplexing Systems." I have examined the final electronic copy of this thesis for form and content and recommend that it be accepted in partial fulfillment of the requirements for the degree of Master of Science, with a major in Electrical Engineering.

Mostofa K. Howlader, Major Professor

We have read this thesis and recommend its acceptance:

Michael J. Roberts, Daniel B. Koch

Accepted for the Council:
Carolyn R. Hodges

Vice Provost and Dean of the Graduate School

(Original signatures are on file with official student records.)

To the Graduate Council:

I am submitting herewith a thesis written by Jaideep Rajan Shahri entitled "Bit loading and peak average power reduction techniques for adaptive orthogonal frequency division multiplexing systems." I have examined the final electronic copy of this thesis for form and content and recommend that it be accepted in partial fulfillment of the requirements for the degree of Master of Science, with a major in Electrical Engineering.

Mostofa K. Howlader

Major Professor

We have read this thesis and
recommend its acceptance:

Michael J. Roberts

Daniel B. Koch

Acceptance for the Council:

Anne Mayhew

Vice Chancellor and
Dean of Graduate Studies

(Original signatures are on file with official student records.)

BIT LOADING AND PEAK AVERAGE POWER REDUCTION TECHNIQUES FOR ADAPTIVE ORTHOGONAL FREQUENCY DIVISION MULTIPLEXING SYSTEMS

A Thesis
Presented for the
Master of Science
Degree
The University of Tennessee, Knoxville

Jaideep Rajan Shahri
August 2004

DEDICATION

This thesis is dedicated to my grand parents, Lalchand and Mani Shahri, and my parents Rajan and Shilpa Shahri, for always believing in me, inspiring me, and encouraging me to reach out and achieve my goals.

ACKNOWLEDGEMENTS

I wish to express my sincere gratitude to my advisor, Dr Mostofa K. Howlader for his ideas, invaluable support, guidance and encouragement through the research. I would also like to thank Dr. Michael J. Roberts and Dr. Daniel B. Koch for serving on my thesis committee.

I wish to thank all those who helped me complete my Master of Science degree in Electrical Engineering.

Finally, I would like to thank my family and friends, for their love, continuous support and whose suggestions and encouragement made this work possible.

ABSTRACT

In a frequency-selective channel a large number of resolvable multipaths are present which lead to the fading of the signal. Orthogonal frequency division multiplexing (OFDM) is well-known to be effective against multipath distortion. It is a multicarrier communication scheme, in which the bandwidth of the channel is divided into subcarriers and data symbols are modulated and transmitted on each subcarrier simultaneously. By inserting guard time that is longer than the delay spread of the channel, an OFDM system is able to mitigate intersymbol interference (ISI).

Significant improvement in performance is achieved by adaptively loading the bits on the subcarriers based on the channel state information from the receiver. Imperfect channel state information (CSI) arises from noise at the receiver and also due to the time delay in providing the information to the transmitter for the next data transmission.

This thesis presents an investigation into the different adaptive techniques for loading the data bits on the subcarriers. The choice of the loading technique is application specific. The spectral efficiency and the bit error rate (BER) performance of adaptive OFDM as well as the implementation complexity of the different loading algorithms is studied by varying any one of the parameters, data rate or BER or total transmit power subject to the constraints on the other two. A novel bit loading algorithm based on comparing the SNR with the threshold in order to minimize the BER is proposed and its performance for different data rates is plotted.

Finally, this thesis presents a method for reducing the large peak to average power ratio (PAPR) problem with OFDM which arises when the sinusoidal signals of the subcarriers add constructively. The clipping and the probabilistic approaches were studied. The probabilistic technique shows comparatively better BER performance as well as reduced PAPR ratio but is more complex to implement.

TABLE OF CONTENTS

Chapter **Page**

LIST OF FIGURES

Figure **Page**

CHAPTER 1
BASIC PRINCIPLES OF ORTHOGONAL FREQUENCY DIVISION MULTIPLEXING

1.1 Introduction

Multiple access techniques represent the most essential functions of access networks, whether based on coaxial cable, fiber, radio, or satellite. Multiple access protocols define how a common resource such as wireless medium is shared among contending users, and hence determine the overall performance of the system. Because of the limited amount of bandwidth available, with the help of multiple access techniques multiple users can share the available spectrum simultaneously. Conventional multiple access techniques include Time Division Multiplexing (TDMA), Frequency Division Multiplexing and Code Division Multiple Access (CDMA). In frequency division multiple access (FDMA), the available frequency band is divided among users in the system. A simple example of FDMA is the use of different frequencies for each frequency modulated radio station. All stations transmit at the same time but do not interfere with each other because they transmit using different carrier frequencies. Additionally they are bandwidth limited and are spaced sufficiently far apart in frequency so that their transmitted signals do not overlap in the frequency domain. At the receiver, each signal is individually received by using a frequency tunable band pass filter to selectively remove all the signals except for the station of interest. This filtered signal can then be demodulated to recover the original transmitted information. FDMA suffers from two drawbacks. First, it requires one bandpass filter per active user and secondly, it is inefficient in terms of channel bandwidth. Orthogonal Frequency Division Multiplexing (OFDM) is very similar to FDMA but it overcomes both of the drawbacks. In OFDM, the data are divided among large number of closely spaced carriers. This accounts for the "frequency division multiplex" part of the name and these carriers are orthogonal to each other, hence the name Orthogonal Frequency Division Multiplexing [1]. All the subcarriers within the OFDM signal are time and frequency synchronized to each other, allowing the interference between subcarriers to be carefully controlled. These multiple

subcarriers overlap in the frequency domain, but do not cause inter-carrier interference (ICI) due to the orthogonal nature of the modulation. The orthogonal packing of the subcarriers also greatly reduces the guard band, improving the spectral efficiency. Each carrier in a FDM transmission can use an analogue or digital modulation scheme. There is no synchronization between the transmissions and so one station could transmit using FM and another in digital using frequency shift keying [2]. In a single OFDM transmission all the subcarriers are synchronized to each other, restricting the transmission to digital modulation schemes. OFDM is symbol based, and can be thought of a large number of low bit rate carriers (not the total bit rate) transmitting in parallel. This is also termed as multicarrier modulation [3]. All these carriers transmit in unison using synchronized time and frequency, forming a single block of spectrum. This is to ensure that the orthogonal nature of the structure is maintained. Since these multiple carriers form a single OFDM transmission, they are commonly referred to as 'subcarriers', with the term 'carrier' reserved for describing the RF carrier mixing the signal from base band. Figure 1.1 illustrates the basic multicarrier modulation transmitting technique, where, R is the total data rate, N is the number of subcarriers, f is the carrier frequency, and $s(t)$ denotes the transmitted signal.

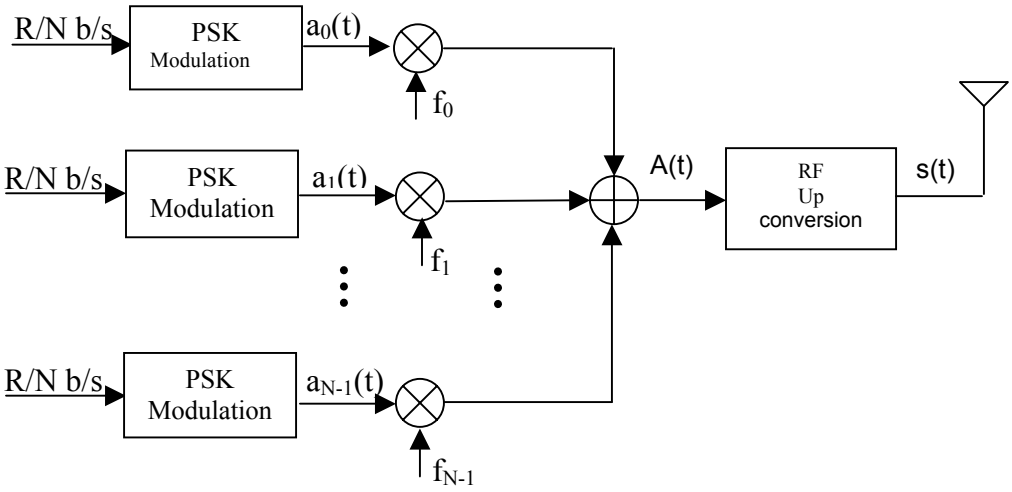

Figure 1.1 Basic multicarrier modulation transmitting technique.

1.2 Orthogonality of Subcarriers

"Orthogonal" is derived from the Greek word "ortho", which means right and "gon" which means angled. This term has been extended to general use to denote the characteristics of being independent. Signals are orthogonal if they are mutually independent of each other, i.e. there is a precise mathematical relationship between the frequencies of the carriers in the system. It allows, multiple information signals to be transmitted perfectly over a common channel and detected, without interference. OFDM signals are made up from a sum of sinusoids, with each corresponding to a subcarrier. The baseband frequency of each subcarrier is chosen to be an integer multiple of the inverse of the symbol time, resulting in all subcarriers having an integer number of cycles per symbol. As a consequence the subcarriers are orthogonal to each other. If τ is the symbol period, then the carriers are linearly independent (i.e. orthogonal) if the carrier spacing is a multiple of $1/\tau$ [4]. Figure 1.2 shows the construction of an OFDM signal with four subcarriers. Sets of functions are orthogonal to each other if they match the conditions in (1.1). For orthogonal functions, if any two different functions within each set are multiplied, and integrated over a symbol period, the result is zero. Another way of thinking of this is that if we look at a matched receiver for one of the orthogonal functions, a subcarrier in the case if OFDM, then the receiver will only see the result for that function. The results from all other functions in the set integrate to zero, and thus have no effect.

$$\int_0^{\tau} s_i(t)s_j(t)dt = \begin{cases} C & i = j \\ 0 & i \neq j \end{cases}. \qquad (1.1)$$

Equation (1.2) shows a set of orthogonal sinusoids, which represent the subcarriers from an unmodulated real OFDM signal.

$$s_k(t) = \begin{cases} \sin(2\pi k f_o t) & 0 < t < \tau, k = 1,2,....N \\ 0 & otherwise \end{cases}, \qquad (1.2)$$

where, f_o is the carrier spacing, N is the number of carriers, τ is the symbol period. These subcarriers are orthogonal to each other; as a result, when we multiply the waveforms of any two subcarriers and integrate over the symbol period, the result is zero. Multiplying

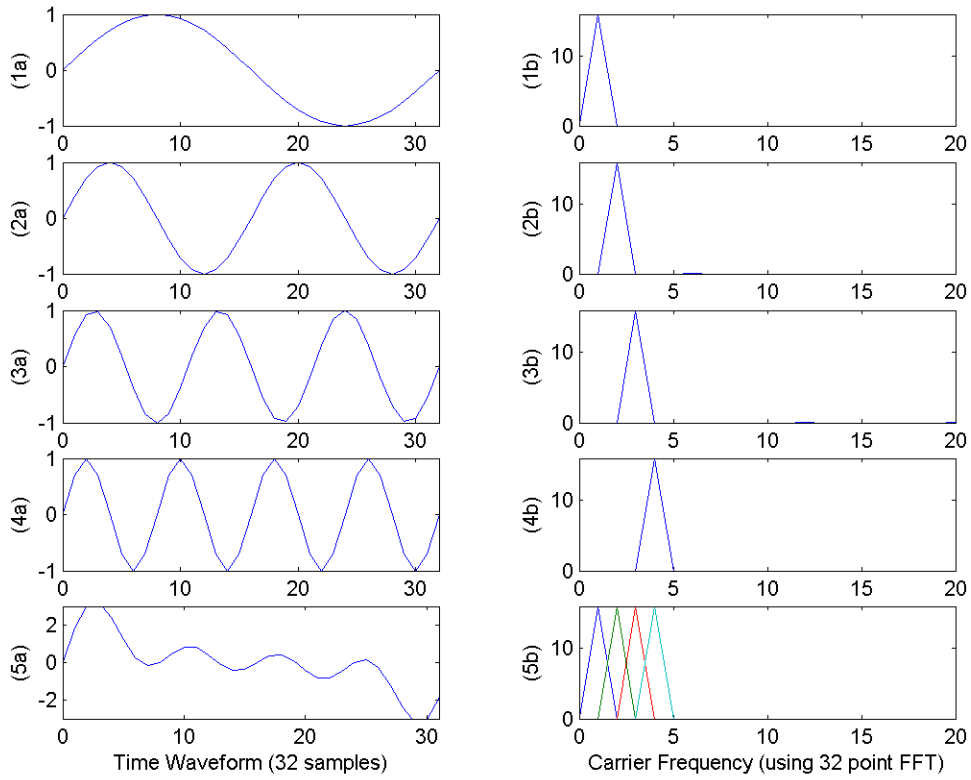

Figure 1.2 Time domain construction of an OFDM signal.

the two sine waves together is the same as mixing the subcarriers. This results in sum and difference of input frequency components, which will always be an integer number of cycles. Since the system is linear, the overall is equivalent to taking the integral of each frequency component separately, and then combining the results by adding the two sub-integrals. The two frequency components after mixing have an integer number of cycles over the period, and so the sub-integral of each component will be zero because the integral of a sinusoid over an entire period is zero. Both the sub-integrals are zero and so the resulting addition of the two will also be zero. Thus we have established that the frequency components are orthogonal to each other. Figures 1.2 (1a), (2a), (3a), and (4a) show individual subcarriers with 1, 2, 3, and 4 cycles per symbol, respectively. The phase on all these subcarriers is zero. Each subcarrier has an integer number of cycles per symbol, making them cyclic. Figures (1b), (2b), (3b), and (4b) show the FFT of the time

waveforms in (1a), (2a), (3a), and (4a) respectively. Figures (5a) and (5b) show the result of the summation for all four subcarriers. Another way to understand the Orthogonality property of OFDM signals is to look at its spectrum [4]. In the frequency domain each OFDM subcarrier has a *sinc*, $\sin(x)/x$, frequency response, as shown in Figure 1.3. This is a result of the symbol time's corresponding to the inverse of the carrier spacing. The rectangular waveform in the time domain results in a *sinc* frequency response in the frequency domain. The *sinc* shape has a narrow main lobe, with many side-lobes that decay slowly with the magnitude of the frequency difference away from the center. Each carrier has a peak at the center frequency and nulls evenly spaced with a frequency gap equal to the carrier spacing. The orthogonal nature of the transmission is a result of the peak of each subcarrier corresponding to the nulls of all other subcarriers. Because an OFDM receiver calculates the spectrum values at the points that correspond to the maxima of the individual subcarriers, it can demodulate each subcarrier free of any interference from all other subcarriers.

1.3 Mathematical Description of OFDM

The mathematical definition of the modulation system helps us see how the signal is generated and how the receiver must operate, and it gives us a tool to understand the effects of imperfections in the transmission channel. As mentioned above, an OFDM signal consists of a sum of subcarriers that are individually modulated using a digital modulation scheme. Each carrier can be described as a complex wave as,

$$s_c(t) = A_c(t)e^{j[\omega_c t + \phi_c t]}, \tag{1.3}$$

where, the real signal is the real part of $s_c(t)$. Both $A_c(t)$ and $\phi_c(t)$, the amplitude and phase of the carrier, can vary on a symbol by symbol basis. The values of the parameters are constant over the symbol duration τ. OFDM consists of many carriers. Thus the complex signal $s_s(t)$ can be represented as,

$$s_s(t) = \frac{1}{N}\sum_{n=0}^{N-1} A_n(t)e^{j[\omega_n t + \varphi_n(t)]}, \tag{1.4}$$

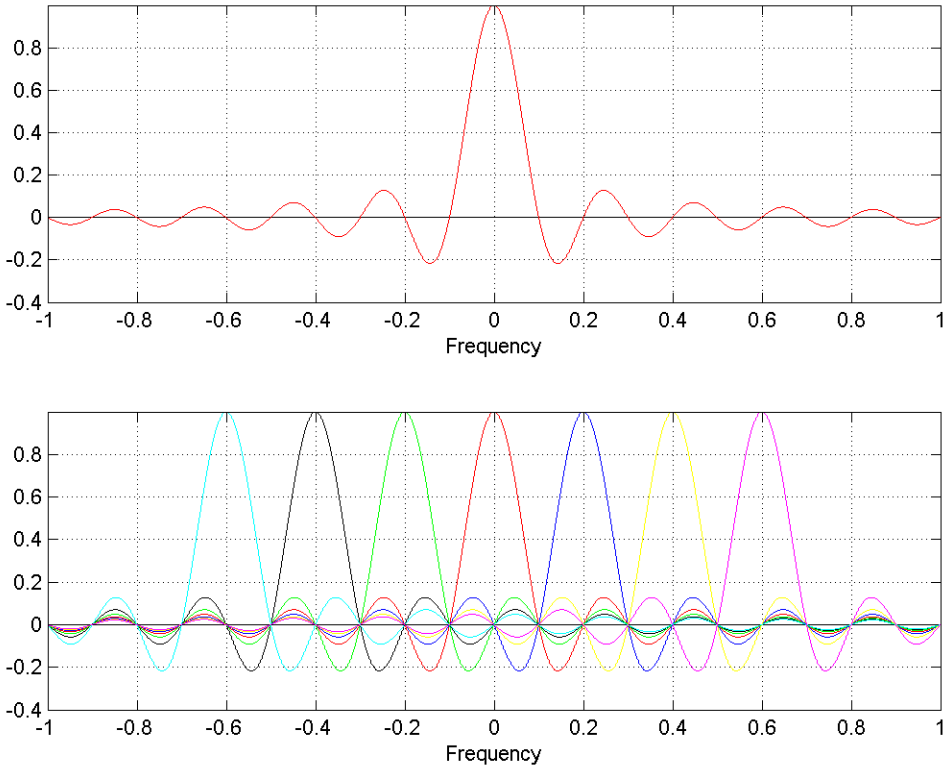

Figure 1.3 Spectra of an OFDM subchannel (top) and an OFDM signal (bottom).

This is of course a continuous signal. If we consider the waveforms of each component of the signal over one symbol period, then the variables $A_c(t)$ and $\phi_c(t)$ take on fixed values, which depend on the frequency of that particular carrier, and so (1.4) can be re-written as,

$$s_s(t) = \frac{1}{N}\sum_{n=0}^{N-1} A_n e^{j[\omega_n t + \phi_n]}. \tag{1.5}$$

If the signal is sampled at a sampling frequency of 1/T, then the resulting signal is represented by,

$$s_s(kT) = \frac{1}{N}\sum_{n=0}^{N-1} A_n e^{j[(\omega_0 + n\Delta\omega)kT + \phi_n]}. \tag{1.6}$$

We also have the relation between the symbol period and the sampling frequency as,

$$\tau = NT. \tag{1.7}$$

If we set $\omega_0 = 0$, then the signal becomes,

$$s_s(kT) = \frac{1}{N}\sum_{n=0}^{N-1} A_n e^{j\phi_n} e^{j(n\Delta\omega)kT}. \tag{1.8}$$

Equation (1.8) can be compared with the general form of the inverse Fourier Transform,

$$g(kT) = \frac{1}{N}\sum_{n=0}^{N-1} G\left(\frac{n}{NT}\right) e^{j2\pi nk/N}. \tag{1.9}$$

The function $A_n e^{j\phi_n}$ is the definition of the signal in the sampled frequency domain and *s(kT)* is the time domain representation. Equations (1.8) and (1.9) are equivalent if,

$$\Delta f = \frac{\Delta\omega}{2\pi} = \frac{1}{NT} = \frac{1}{\tau}\ . \tag{1.10}$$

This is the same condition that was required for orthogonality explained in Section 1.2. Thus, one consequence of maintaining orthogonality of is that the OFDM signal can be defined by using Fourier transform procedures [1].

1.4 Generation of OFDM using Discrete Fourier Transform

The definition of N-point discrete Fourier transform (DFT) is,

$$X_p[k] = \sum_{n=0}^{N-1} x_p[n] e^{-j(2\pi/N)k_n}, \tag{1.11}$$

and the N-point inverse discrete Fourier Transform (IDFFT) is,

$$x_p[n] = \frac{1}{N}\sum_{k=0}^{N-1} X_p[k] e^{j(2\pi/N)k_n}. \tag{1.12}$$

We know that the sinusoids of the DFT form an orthogonal basis set and a signal in the vector space of the DFT can be represented as a linear combination of orthogonal sinusoids. One view of the IDFT is that the transform essentially correlates its input signal with each of its sinusoidal basis functions. If the input signal has some energy at a certain frequency, there will be a peak in the correlation between the input signal and the basis sinusoid at that corresponding frequency. Now this transform is used to map the input symbols onto a set of orthogonal subcarriers i.e. to the orthogonal basis functions of the DFT. Consider a data sequence (d_0,d_1,d_2,…d_{n-1}), where each d_n is a complex number

$d_n=a_n+jb_n$. (a_n, $b_n=\pm 1$ for QPSK, a_n, $b_n=\pm 1,\pm 3$ for 16QAM …). So at the receiver we get the signal as,

$$D_k = \sum_{n=0}^{N-1} d_n e^{-j(2\pi nk/N)} = \sum_{n=0}^{N-1} d_n e^{-j2\pi f_n t_k} \qquad k = 0,1,2,..., N-1 \tag{1.13}$$

where, $f_n = n/(N\Delta t), t_k = k\Delta t$ and Δt is an arbitrarily chosen symbol duration of the serial data sequence d_n. The real part of the vector D has components,

$$Y_k = \mathrm{Re}\{D_k\} = \sum_{n=0}^{N-1} [(a_n \cos(2\pi f_n t_k) + b_n \sin(2\pi f_n t_k))], \qquad k = 0,1,..., N-1. \tag{1.14}$$

If these components are applied to a low pass filter at time intervals Δt, a signal is obtained that closely approximates the frequency division multiplexed signal.

$$y(t) = \sum_{n=0}^{N-1} [a_n \cos(2\pi f_n t_k) + b_n \sin(2\pi f_n t_k)], \quad 0 \le t \le N\Delta t. \tag{1.15}$$

Thus, the hardware implementation which makes use of multiple modulators and demodulators, which was impractical, has been overcome by the ability to generate the signal using the inverse Fourier transform. Figure 1.4 illustrates the process of a typical FFT/IFFT based OFDM system. The incoming serial data stream is first converted to a parallel stream of bits and grouped into *x* bits each to form a complex number. The number *x* determines the signal constellation of the corresponding subcarriers, such as 4-, 8-, 16-, 32-, 64- or 128- PSK or QAM. The complex numbers are modulated in a baseband fashion by the IFFT and converted back to serial data for transmission. A guard interval is inserted between symbols to avoid intersymbol interference and intercarrier interference caused by multipath distortion. The discrete symbols then are converted to analog, put on the carrier and sent to the receiver through the channel. The receiver performs the reverse process of the transmitter. The carrier is removed from the received signal and then baseband analog signal is converted back to digital and guard interval is removed. After this, the signal is converted into parallel branches and an FFT is performed which converts the received signal back into the baseband complex-mapped symbols. These complex symbols are then demapped and converted into serial streams of bits [3].

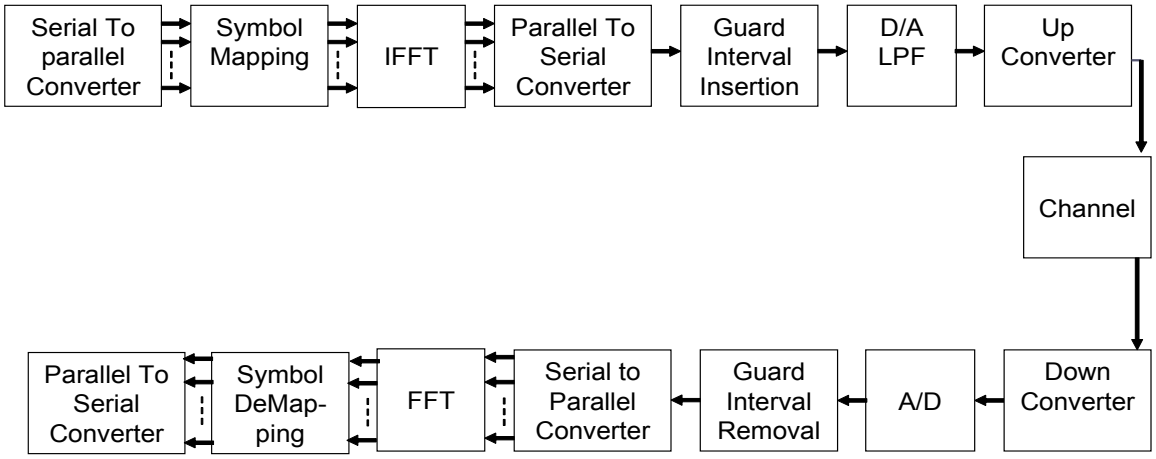

Figure 1.4 FFT/IFFT based OFDM system.

1.5 Guard Interval and its Implementation

The orthogonality of a subcarrier with respect to other subcarriers is lost if the subcarrier has non-zero spectral value at other subcarrier frequencies. From the time domain perspective, the corresponding sinusoid no longer has an integer number of cycles within the FFT interval. Figure 1.5 shows the spectra of four subcarriers in the frequency domain when they are orthogonal to each other and when orthogonality is lost.

The orthogonality of subchannels can be maintained when there is no intersymbol interference (ISI) and the intercarrier interference (ICI) introduced by the fading channel. In practice these conditions cannot be obtained since the spectrum of an OFDM signal is not strictly band limited (*sinc(f)* function), and linear distortion such as multipath causes ISI. Multipath propagation is caused by the radio transmission signal reflecting off objects in the propagation environment, such as walls, buildings etc. These multiple signals arrive at the receiver at different times due to the transmission distances being different. This causes each subchannel to spread energy into adjacent channels. This situation can be viewed from the time domain perspective, in which the integer number of cycles for each subcarrier within the FFT interval of the current symbol is no longer maintained due to the phase transition introduced by the previous symbol. Finally, any offset between the subcarrier frequencies of the transmitter and receiver also introduces ICI in an OFDM

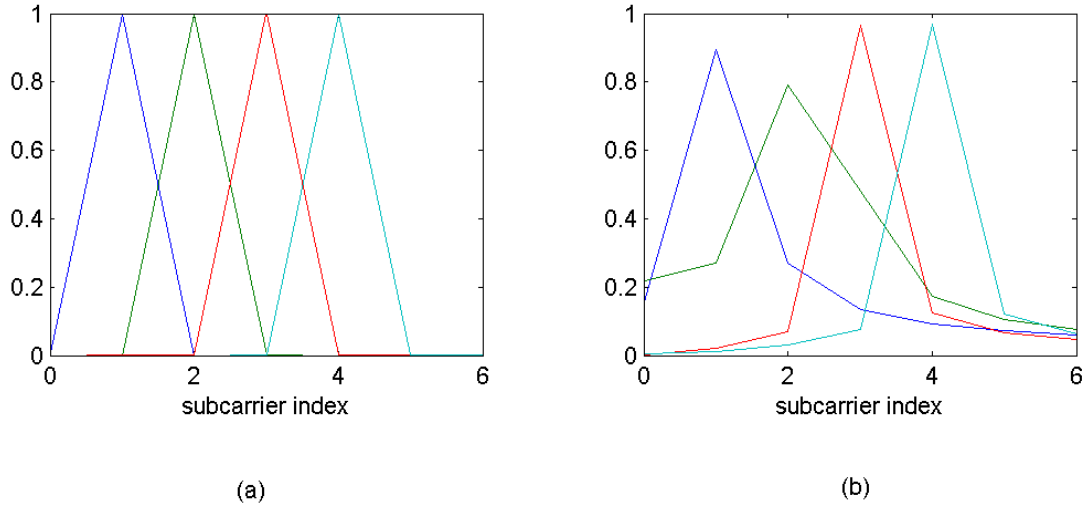

Figure 1.5 Spectra of four (a) orthogonal and (b) non-orthogonal subcarriers.

symbol. Increasing the symbol duration or the number of carriers so that distortion becomes insignificant may sound like a simple solution but it is difficult to implement in terms of carrier stability and the FFT size. For an OFDM transmitter with N subcarriers, if the duration of a data symbol is T', the symbol duration of an OFDM symbol at the output of the transmitter is,

$$T_{sym} = T'N. \tag{1.16}$$

Thus if the delay spread of a multipath channel is greater than T' but less than T_{sym}, the data symbol in the serial data stream will experience frequency-selective fading while the data symbol on each subcarrier will experience only flat-fading. This low data symbol rate makes OFDM naturally resistant to effects of ISI.

The effect of ISI on an OFDM signal can be further improved by the addition of a guard period to the start of each symbol before transmission and removed at the receiver before the FFT operation. If the guard time is chosen such that its duration is longer than the delay spread, the ISI can be eliminated. The total symbol duration is $T_{total}=T_g+T$, where T_g is the guard interval and T is the symbol duration. Since the insertion of a guard interval will reduce data throughput, T_g is usually less than T/4 [5]. Figure 1.6 illustrates the concept of guard time insertion to eliminate ISI for an OFDM symbol. As seen, the OFDM symbol received from the direct path is interfered by the previous OFDM symbol

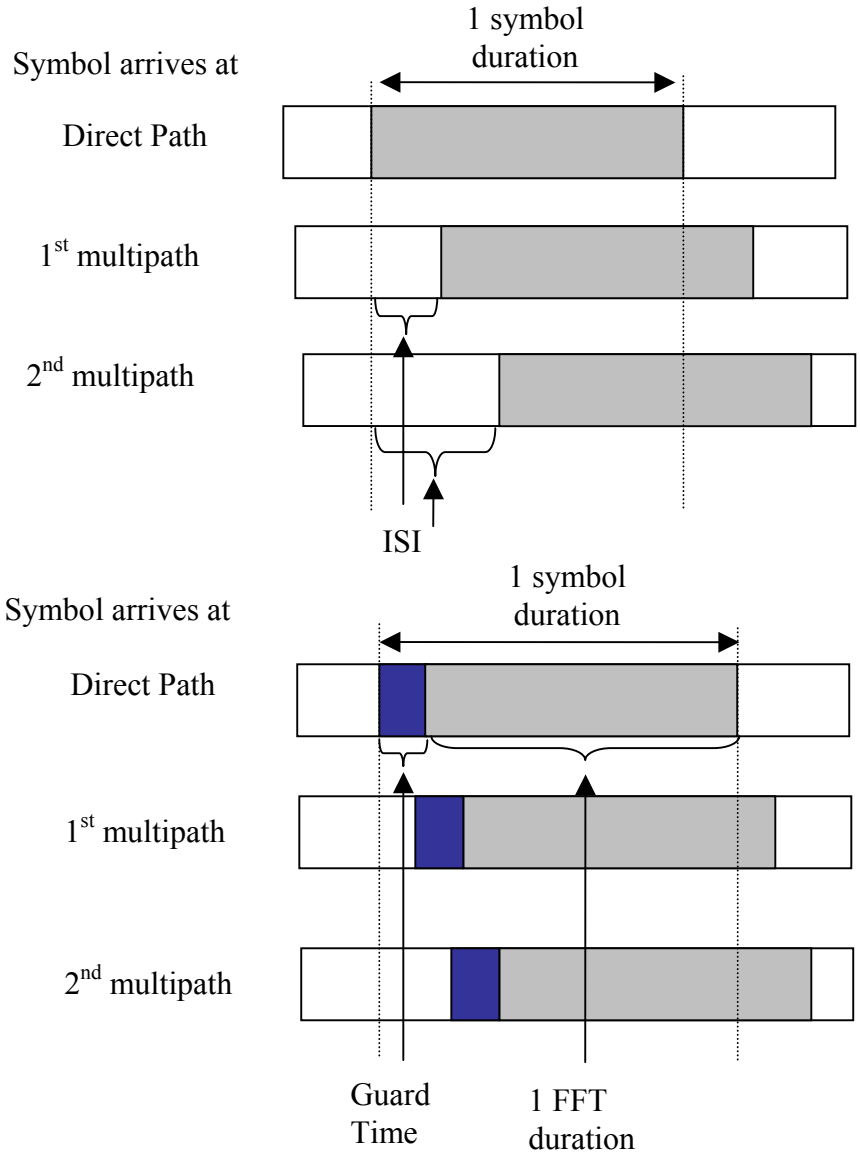

Figure 1.6 Received OFDM symbols after passing through a multipath channel without guard time and with guard time.

received from the first and second multipaths. As long as the delay spread is shorter than the guard interval, ISI is avoided. However, the received symbol is still interfered by its replicas and we refer to this type of interference as self interference or intercarrier interference (ICI). The ratio of the guard interval to useful symbol duration is application dependent.

To eliminate ICI, a cyclic copy is used as guard interval. The end of the symbol is copied and appended to the start and thus gets a cyclically extended block and a longer symbol time. If an OFDM block is represented as $a = [a_0, a_1, ..., a_{N-1}]$, an OFDM block with cyclic prefix k would be represented as $a' = [a_{N-k}, a_{N-k+1}, ..., a_N, a_0, a_1, ..., a_{N-1}]$. The cyclic prefix causes the sequence of $\{a_k\}$ to appear periodic to the channel and clears the channel memory at the end of each input block. This action makes successive OFDM block transmissions independent. In other words, a cyclic prefix ensures that delayed replicas of the same OFDM block should always have an integer number of cycles within the FFT interval. As explained above, the influence of ISI can be reduced by increasing the duration of an OFDM symbol. To quantify the influence we define a measure as,

$$\eta = \frac{delay \quad spread}{symbol \quad duration}. \tag{1.17}$$

For a given bandwidth of an OFDM signal, the symbol duration is proportional to the number of subcarriers. If η is large, a significant number of samples of individual OFDM symbols are affected by ISI and the system will have a high BER. On the other hand, if η is small, a small portion of the individual OFDM symbols is affected by ISI and thus the system will have a low BER. Also, for a given signal bandwidth, the frequency spacing between subcarriers decreases as the number of subcarriers increases. The small frequency separation between two subcarriers makes them more vulnerable to ICI due to the frequency offset introduced by the Doppler spread of the channel. Figure 1.7 shows the bit error rate performance versus the maximum delay spread for an OFDM system with 64 subcarriers. The symbol duration is 3.2 μs . Three different guard times of

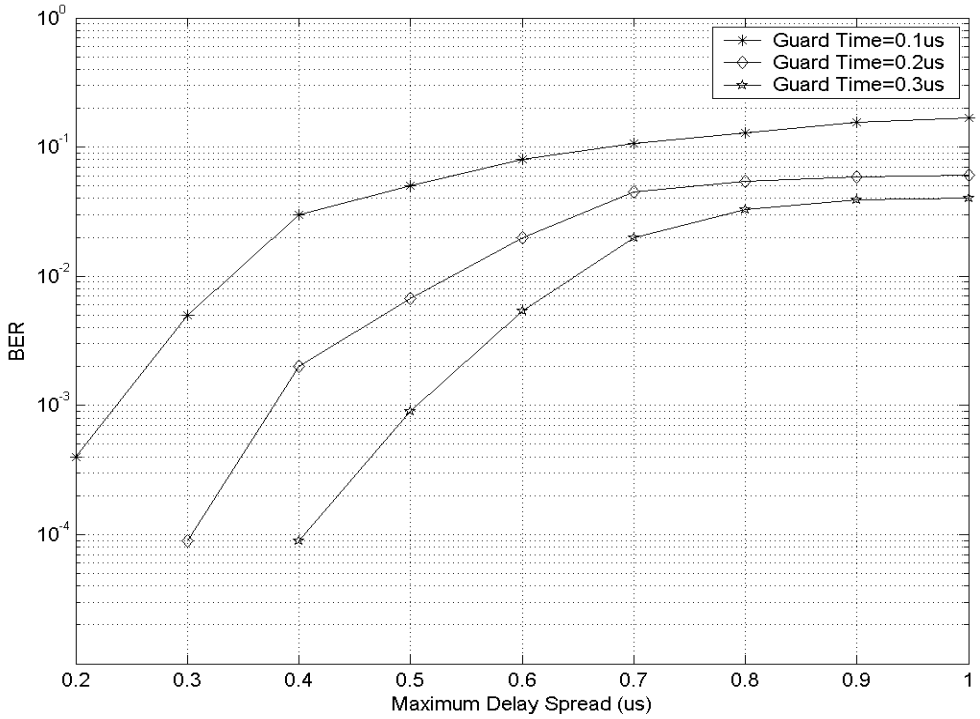

Figure 1.7 BER versus delay spread for 64 subcarrier OFDM system with different guard time.

0.1, 0.2 and 0.3 μs are studied. Simulation results show that for the case of maximum delay spread less than guard time, no error is produced at the receiver. Once the delay spread exceeds the guard time, ISI is introduced. The BER increases rapidly at the beginning and then gradually approaches an error floor as the effect of guard time to the delay spread on the performance becomes insignificant [6].

1.6 Effect of Additive White Gaussian Noise on OFDM

Noise exists in all communication systems operating over a physical channel. The main sources of noise are thermal background noise and electrical noise in the receiver amplifiers. In addition to this, noise can be internally generated, as explained in the previous sections, as a result of intersymbol and intercarrier interference.

These sources of noise decrease the signal-to-noise ratio (SNR), ultimately limiting the spectral efficiency of the system. Most types of noise present in communication systems can be modeled using additive white Gaussian noise (AWGN). This noise has uniform spectral density (making it white), and a Gaussian distribution in amplitude. Thermal and electrical noise, primarily have white Gaussian noise properties, allowing them to be modeled accurately with AWGN. OFDM signals have a flat spectral density and a Gaussian amplitude distribution, because of this the intercarrier interference from other OFDM symbols have AWGN properties.

1.6.1 Modulation Schemes

Digital data are transferred in an OFDM link by using a modulation scheme on each subcarrier. A modulation scheme is a mapping of data words to a real and imaginary constellation, also known as IQ constellation. The number of bits that can be transferred using a single symbol corresponds to $\log_2(M)$, where M is the number of points in the constellation. As the bandwidth of transmission is fixed, using a modulation scheme with a large number of constellation points allows for improved spectral efficiency. The greater the number of points in the modulation constellation, the harder they are to resolve at the receiver. As the IQ locations become spaced closer together, it only requires a small amount of noise to cause errors in the transmission.

1.6.2 Calculation of OFDM Parameters

For a given bit rate R and the delay spread of a multipath channel τ, the parameters of OFDM are determined as in given in [3], [6]. The guard time G should be at least twice the delay spread, i.e.

$$G \geq 2\tau . \tag{1.18}$$

To minimize the SNR loss due to the guard time, the symbol duration should be much larger than the guard time. However, symbols with large time duration are susceptible to Doppler spread, phase noise and frequency offset. As a rule of thumb, the OFDM symbol duration T_{sym} should be at least five times the guard time, i.e.

$$T_{sym} \geq 5G . \tag{1.19}$$

The frequency spacing between two adjacent subcarriers Δf is,

$$\Delta f = \frac{1}{T_{sym}}. \tag{1.20}$$

For a given data rate R, the number of information bits per OFDM symbol B_{inf} is,

$$B_{\inf} = RT_{sym}. \tag{1.21}$$

For a given B_{inf} and number of bits per symbol per subcarrier R_{sub}, the number of subcarriers N is,

$$N = \frac{B_{\inf}}{R_{sub}}, \tag{1.22}$$

where R_{sub}= 2 bits/symbol/subcarrier for QPSK and so on. The OFDM bandwidth is defined as,

$$BW = N\Delta f. \tag{1.23}$$

Thus we see that, increasing the symbol duration decreased the frequency spacing between subcarriers. So, for a given signal bandwidth, more subcarriers can be accommodated. On the other hand, for a given number of subcarriers, increasing the symbol duration decreases the signal bandwidth. Using these parameters we have plotted the BER performance of an OFDM system in the next subsection.

1.6.3 OFDM versus Single Carrier Transmission

The BER of an OFDM system is dependent on several factors, such as the modulation scheme used, the amount of multipath, and the level of noise in the signal. The performance of OFDM with just AWGN is exactly the same as that of a single carrier coherent transmission scheme. For a single carrier transmission that is modulated and transmitted, the transmitted amplitude and phase are held constant over the period of the symbol and are set based on the modulation scheme and transmitted data. This results in a *sinc* frequency response which is the response for OFDM. The receiver for single carrier transmission uses an integrate and dump method which averages the received IQ vector over the entire symbol, then performs IQ demodulation on the average. The demodulation of an OFDM signal is preformed in the same manner. In the receiver an FFT is used to estimate the amplitude and phase of each subcarrier. The FFT operation is

exactly equivalent to IQ mixing each of the subcarriers to DC then applying an integrate and dump over the number of samples. From this we can see that FFT performs the same operation as the matched receiver for the single carrier transmission, except now for a bank of subcarriers. From this we conclude that in AWGN, OFDM will have the same performance as a single carrier transmission.

Figure 1.8 shows the plot of bit error rate (BER) versus Eb/No using different modulation levels, where *Eb* is the energy per bit and *No* is twice the noise power spectral density. As the channel is considered to be AWGN , therefore the delay spread of a multipath fading channel is not considered here. QPSK, 8-, 16-, 32- and 64- PSK modulation levels were used on 64 carriers in one OFDM block. The carrier frequency was 5 GHz. The BER performance decreases as the modulation level increases. This is due to the fact that as the constellation size increases, the size of the decision region decreases. Hence, chances of errors become more likely to occur with the increase in the number of constellation points. Also, in order to get a certain level of BER, Eb/No increases as the number of bits per symbol increases [7].

Most propagation environments suffer from the effects of multipath propagation. For a given fixed transmission bandwidth, the symbol rate for a single carrier transmission is very high, where as for an OFDM signal it is the number of subcarriers used times lower. This lower symbol rate results in lowering ISI. Also use of guard period removes any ISI shorter than its length.

The adaptive modulation technique discussed in the next chapter varies the modulation technique per the channel variations and as a result greater average spectral efficiency is obtained and performance of adaptive OFDM in multipath environment is similar to performance in AWGN channel. However, the performance of a single carrier transmission will degrade rapidly in the presence of multipath.

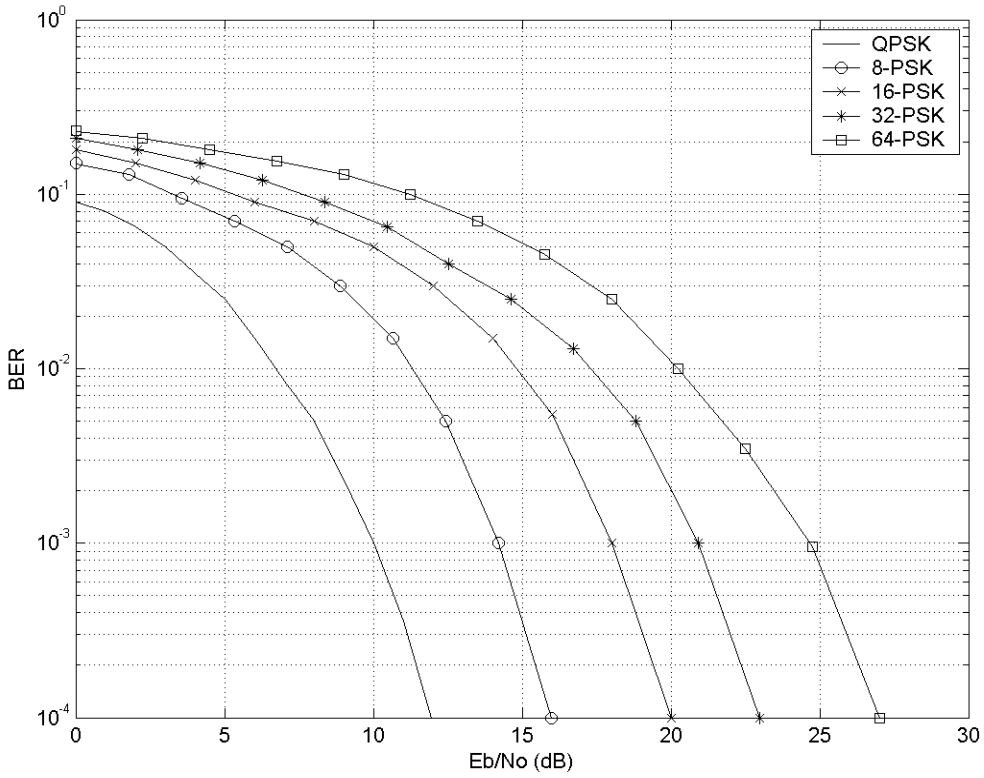

Figure 1.8 BER performance of OFDM system in AWGN.

1.7 Outline of the Thesis

Having studied the usefulness of OFDM and its basic fundamentals, we realized the robustness of OFDM against multipath distortion compared to single carrier systems. We now need to focus on extracting optimal performance i.e. maximum spectral efficiency and minimum BER. Chapter 2 focuses on explaining the concepts of adaptive OFDM in order to maximize performance. The important role played by the accuracy in the channel state information is stressed. We are well aware of the fact that if we increase the data rate, the number of bits in error would increase so depending on the application to be used in, we need to adaptively load the bits on the subcarrier either to increase the data rate or minimize the error rate or minimize the transmit power. More bits are sent on carriers with good frequency response and lesser bits on carriers with poor response. Chapter 3 investigates the different bit loading algorithms. We have compared the

performance of different loading techniques using various modulation scheme combinations and different bit rates. When the subcarriers add constructively, spurious high amplitude peaks in the composite time signals occur; Chapter 4 studies the techniques to reduce the large envelope fluctuation. The clipping and the probabilistic approach using the random phase shifting are focused on. The BER performance as well as the reduction in the peak to average ratio using these techniques is compared. Finally, Chapter 5 concludes the thesis with the contributions as well as the future work that can be explored in this area.

CHAPTER 2
ADAPTIVE OFDM

2.1 Need for Adaptive OFDM

We have seen in Chapter 1 that due to longer symbol period on each subcarrier, the OFDM signal is more robust against large multipath delay spreads that are normally encountered in wireless environments when compared with single carrier transmission. Multipath propagation results in frequency selective fading that leads to fading of individual subcarriers. In addition to this, interference from neighboring carriers can cause the SNR to vary significantly over the system bandwidth. In mobile radio channels, the Rayleigh distribution is commonly used to describe the statistical time average varying nature of the received envelope of a flat fading signal or the envelope of an individual multipath component. Figure 2.1 shows plot of BER versus the SNR in Rayleigh fading channel, where, 64 subcarriers were used with QPSK, 8-, 16-, 32- and 64- PSK modulation levels. The carrier frequency was 5 GHz and the maximum delay spread was considered to be $0.8\,\mu s$. It is observed that in order to attain a certain level of BER, a greater E_b/N_o is required compared to when in AWGN. This is due to the fast fading channel that continuously varies in time and some parts of the transmitted signal experience deep fades and will have poor SNR resulting in a high overall BER. These poor error rates can be mitigated by coding and diversity [8]. Another technique for improving the performance is adaptive OFDM, whereby the modulation levels of the subcarrier is varied as a function of the channel response. When the channel attenuation is high, a lower order modulation level is used and vice versa when the channel response is good [9].

Work in this chapter, demonstrates the effectiveness of using adaptive OFDM and also provides an insight of the requirements at the transmitter and receiver to implement adaptive modulation.

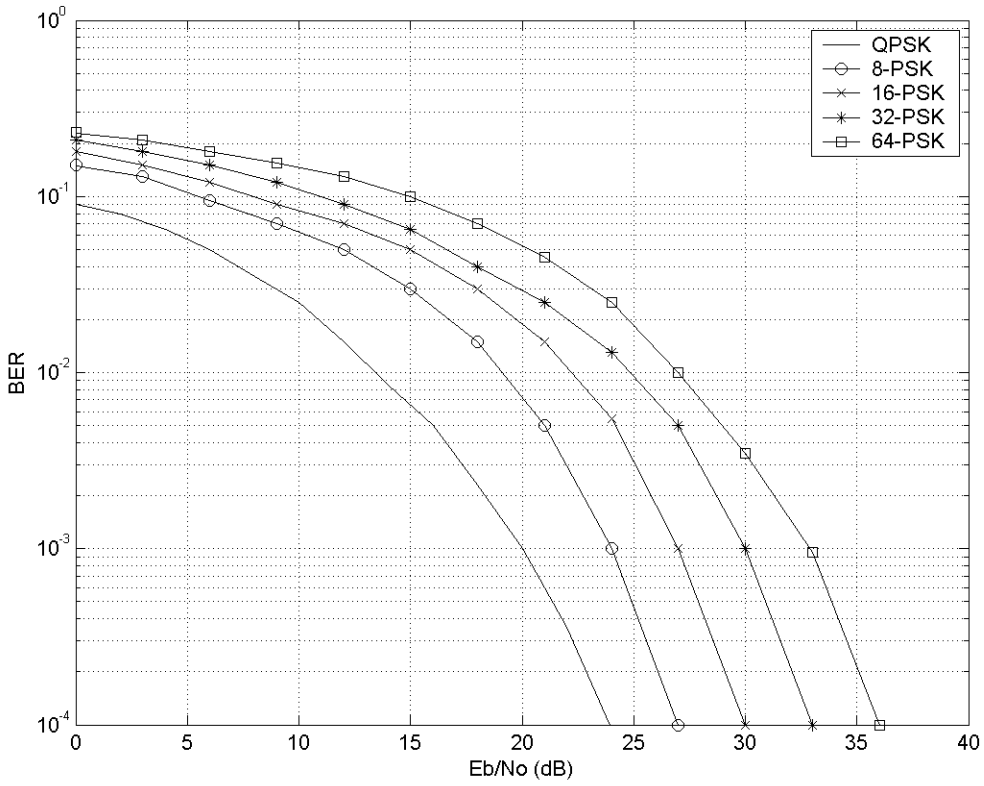

Figure 2.1 BER performance of OFDM system in multipath Rayleigh fading channel.

2.2 Steps Involved in Adaptive OFDM

Varying the modulation levels on individual subcarriers in adaptive OFDM is an action of the transmitter in response to the time varying channel conditions. This parameter adaptation is only suitable when the communication between the transmitter and the receiver is duplex, as it relies on channel estimation and signaling. In order to efficiently react to the changes in the channel quality, the following steps have to be taken:

A. Channel Quality Estimation.

In order to select the transmission parameters to be employed for the next transmission, a reliable prediction of the channel quality during the next active transmit timeslot is necessary.

B. Choice of the Appropriate Parameters for the Next Transmission

Based on the prediction of the expected channel conditions during the next timeslot, the transmitter has to select the appropriate modulation schemes for the subcarriers.

C. Signaling

The receiver has to be informed, as to which set of demodulator parameters to employ for the received packet. This information can either be conveyed within the packet, at the cost of loss of useful bandwidth, or the receiver can attempt to estimate the parameters employed at the transmitter by means of blind detection mechanisms. We see that estimating the channel state information plays the foremost role in maximizing the channel capacity by suitably adapting the transmission parameters [10], [11]. Let us study each of these steps in detail.

2.3 Channel State Information

Channel State Information is the knowledge or estimate of the time varying channel. It is obtained with the help of various channel estimators. The channel estimators evaluate the channel response and help in signaling the transmitter. Based on the signal which is usually in the form of pilot tones or special training symbols, the transmitter can adapt the channel transmission parameters. The channel estimators are a part of the receiver. There are several different types of channel estimators. They are discussed below.

A. Two Dimensional Channel Estimator

Generally, radio channels undergo fading in both the time and frequency domains. Hence, a channel estimator has to estimate time varying amplitudes and phases of all subcarriers. A two dimensional estimator is successful in correctly determining the channel response based on the effect of the channel variation on a few known pilot tones or symbol. The receiver knows the position of the pilot tones and, based on these references, all other values can be estimated by performing a two dimensional

interpolation. Figure 2.2 shows a transmission of 8 OFDM blocks with 10 subcarriers in each block. Three pilot tones shown in gray are sent in each block [12], [13].

B. One Dimensional Channel Estimator

In this channel estimation technique, instead of directly calculating the two dimensional interpolation, it is possible to separate the interpolation into two one-dimensional interpolations. First an interpolation in the frequency domain is performed for all pilot symbols in all transmitted blocks and that is then repeated in time domain to estimate the remaining channel values.

C. Special Training Symbols

Instead of sending pilot tones in every OFDM block, this technique involves sending several OFDM blocks as reference or pilot. This method is shown in Figure 2.3. 8 OFDM blocks with 10 subcarriers in each block are sent. The first two blocks are the preamble for which all data values are known. These training symbols are then used to obtain the channel estimates.

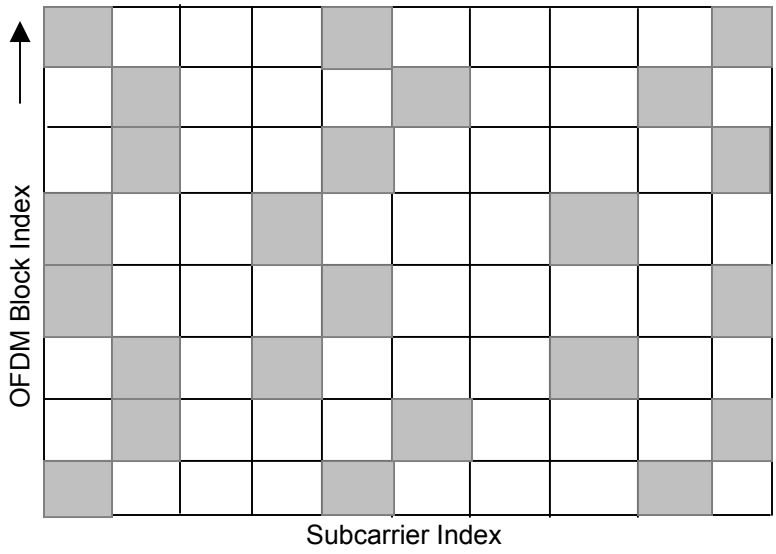

Figure 2.2 Transmission of 8 OFDM blocks each with 10 subcarriers, pilot tones are marked in grey.

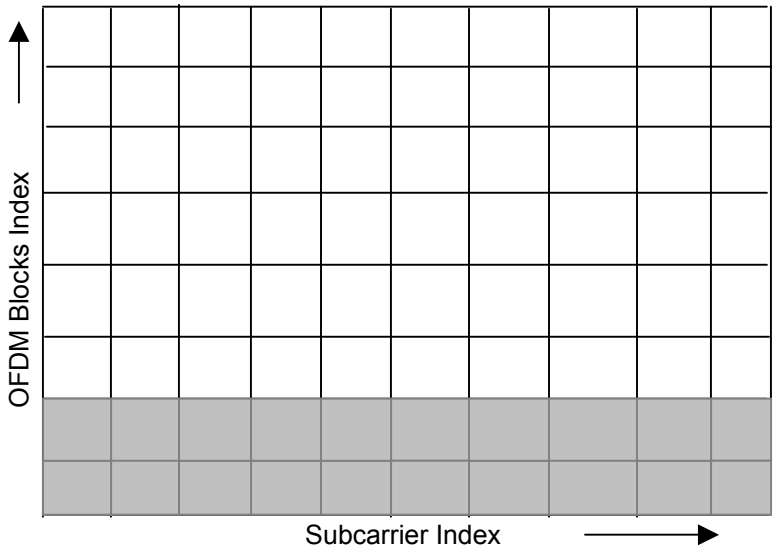

Figure 2.3 Packet transmission with first two training blocks for channel estimation.

D. Decision Directed Channel Estimation

In this technique, instead of pilot tones, data estimates are used to demodulate the symbols from the received subcarriers, after which all subcarriers can be used to estimate the channel. It is not possible to make reliable decisions before a good channel estimate is available. Therefore, only decisions from the previous block are used to predict the channel in the current symbol. This is in contrast to the pilot methods, where the channel for a certain block is estimated from the pilots that were transmitted in the block before. In order to start the decision directed channel estimation, at least one known OFDM block must be transmitted. This enables the receiver to obtain channel estimates for all subcarriers, which are then used to detect the data in the following OFDM block. Once data estimates are available for a block, these estimates ate used to de-map and detect the symbols from the subcarriers and after which those subcarrier values can be used as pilots in exactly the same way as described in the channel estimations in type A and B [10].

2.4 Choice of Transmission Parameters

On receiving the channel state information, the transmitter has to accordingly vary the transmission parameters. There are several adaptive loading algorithms which define the steps involved in adaptively loading the bits on the subcarriers so as to maximize the spectral efficiency, improve the BER performance and minimize the total power. More bits are loaded on the subcarriers with high SNRs and fewer or no bits are sent on subcarriers with high attenuation, low SNR. The rate adaptive algorithm maximizes the spectral efficiency while keeping the total power and the probability of error constant. The fixed throughput algorithm minimizes the BER while keeping the data rate and the total power constant. The power adaptive algorithm minimizes the total power keeping the data rate and the probability of error constant. Figure 2.4 shows the bit loading algorithm, which assigns more bits to subcarriers with high frequency response values, for a sample frequency response of a multipath Rayleigh fading channel. In this example, there are 16 subcarriers in one block and an average of two bits per subcarrier or a total of thirty two bits in every block. The dotted line shows the normalized value of the channel frequency response while the solid line represents the number of bits assigned to each subcarrier [14].

2.5 Signaling

In order for the transmitter to get the channel estimate, the receiver and the transmitter must communicate with each other without any problem or disruption. In order to achieve this, two main types of data transmission techniques are used.

A Time Division Duplex (TDD) System

In this type of data transmission system, the communication between the transmitter and the receiver is bi-directional and the channel is considered reciprocal. There is no extra feedback path from the receiver to the transmitter. The channel quality estimation for each link can be extracted from the reverse link. This method is referred to as open loop adaptation. The transmitter needs to communicate the transmission parameters to the receiver or the receiver can attempt blind detection of the parameters.

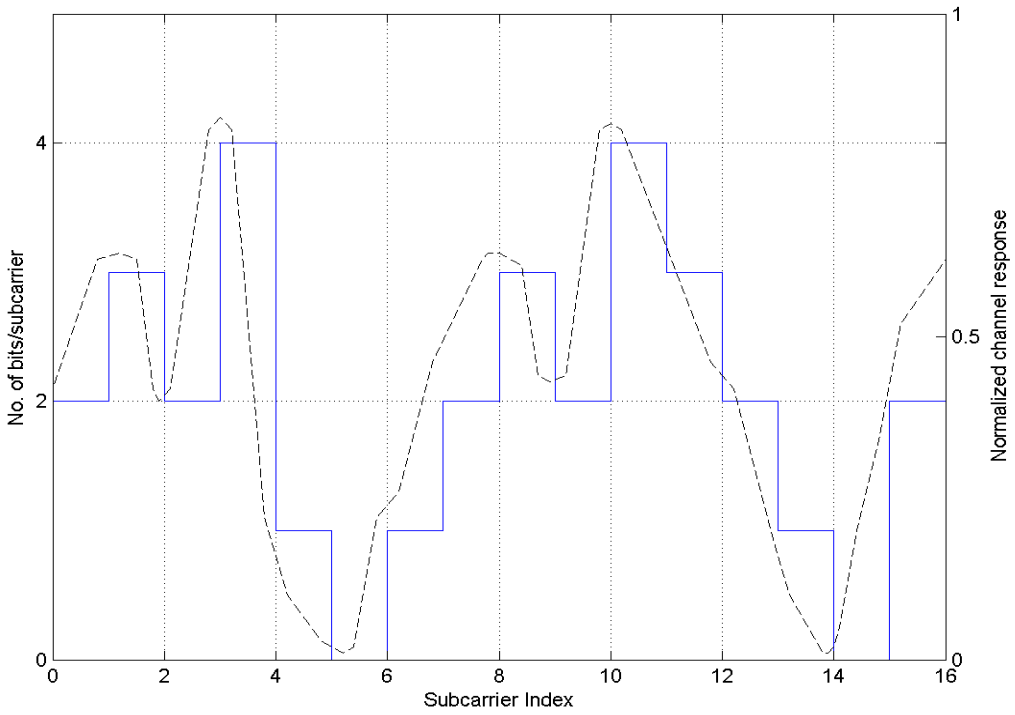

Figure 2.4 Example of bit loading algorithm.

B Frequency Division Duplex (FDD) System

This system is used when the channel is not reciprocal as in case of separate up and down link communication systems. The channel quality measure or the set of the set requested transmission parameters is communicated to the transmitter in the reverse link. It is also referred to as closed-loop adaptation. The transmitter and the receiver cannot determine the bit loading parameters for the next block from the previously received blocks. The receiver has to estimate the channel quality and signal the channel state information to the transmitter via the feedback path. This path is implemented by establishing a low rate signaling channel from the receiver to the transmitter.

2.6 Adaptive OFDM Block Diagram

The block diagram of an OFDM system using adaptive modulation is shown in Figure 2.5. As seen we are using FDD system with an ideal feedback channel from the

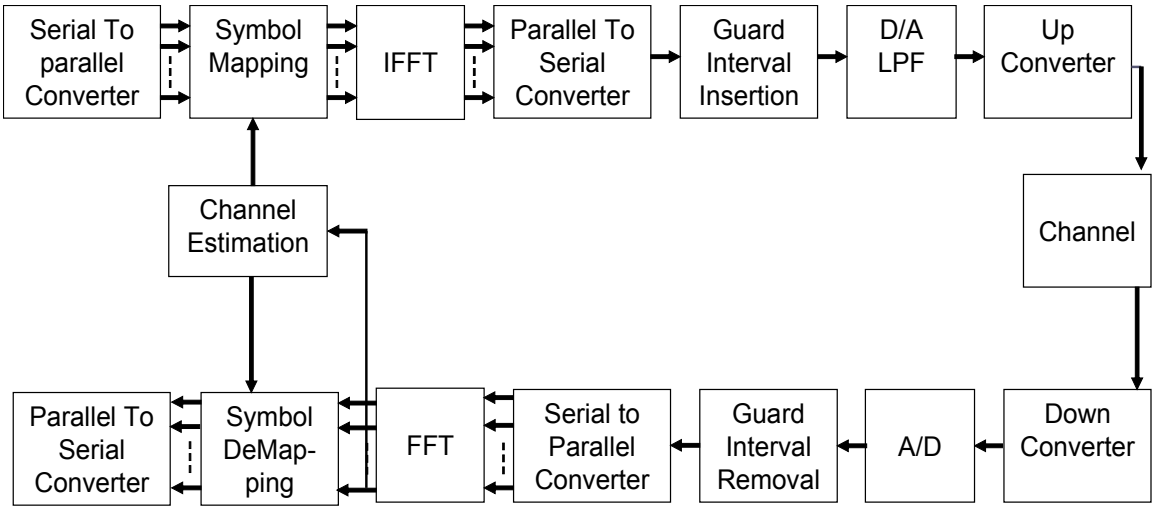

Figure 2.5 Block Diagram of FFT/IFFT based adaptive OFDM system.

receiver to the transmitter. At the transmitter, input bits are loaded adaptively onto all the subcarriers according to their corresponding channel responses. The bits allocated to every subcarrier are then, using the modulation schemes, mapped to the corresponding constellation size to generate a complex symbol. These symbols in all subcarriers form an OFDM block and are transformed into the time domain using IFFT. A guard interval is added to the entire block to prevent ISI. The block is then transmitted to the receiver via channel. At the receiver the guard interval is first removed and the signal is converted into parallel branches of signals and an FFT converts those signals back into frequency domain [10].

2.7 Usefulness of Adaptive OFDM

Figure 2.6 shows an example of applying adaptive modulation to an individual subcarrier as the channel SNR varies with time. Adaptive modulation has a number of key advantages over fixed modulation in every OFDM block. In systems that use a fixed modulation scheme the subcarrier modulation must be designed to provide an acceptable BER under the worst channel conditions. This results in most systems using BPSK or QPSK modulation schemes. However these modulation schemes give a poor spectral efficiency (1-2 b/s/Hz) and result in an excess link margin most of the time.

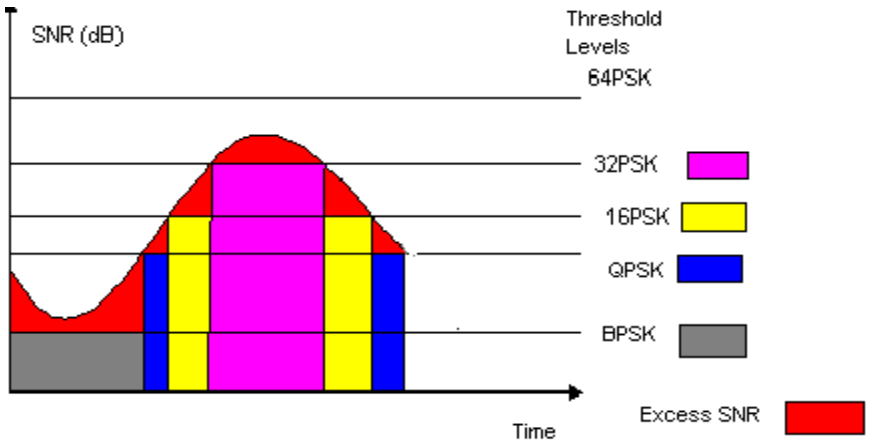

Figure 2.6 Adaptive modulation based on the SNR of the channel. Excess SNR results in the BER being lower than the threshold.

Using adaptive modulation, the remote stations can use a much higher modulation level when the channel is good i.e. high frequency response. Thus the modulation level can be increased from BPSK (1 b/s/Hz) up to 16 QAM - 256 QAM (4 - 8 b/s/Hz), significantly increasing the spectral efficiency of the overall system. Using adaptive modulation can effectively control the BER of the transmission, as the subcarriers that have a poor SNR can be allocated a low modulation scheme such as BPSK or none at all, rather than causing large amounts of errors with a fixed modulation scheme. This significantly reduces the need for forward error corrections [15].

2.8 Limitations of Adaptive OFDM

There are several limitations with adaptive modulation. Overhead information needs to be transferred, as both the transmitter and receiver must know what modulation is currently being used. Also as the mobility of the remote station is increased, the adaptive modulation process requires regular updates, further increasing the overhead. There is a tradeoff between the power control and adaptive modulation. If a remote station has a good channel path the transmitted power can be maintained and a high

modulation scheme used, or the power can be reduced and the modulation scheme reduced accordingly. Another issue is the imperfect channel state information reaching the transmitter from the receiver. Imperfect channel information arises from the limitation of channel estimators as well as outdated information due to time varying channel conditions. The issue with imperfect channel condition can be dealt by considering an estimation of the channel condition at the transmitter and then suitably adapting the transmission parameters [4]. This has been dealt in the next section.

2.9 Imperfect Channel State Information

We are using a frequency-division duplex system, in which a separate feedback channel is used by the receiver to convey the channel response to the transmitter. Due to noise at the receiver itself, certain limitations are imposed on the performance of channel estimators and so there is inaccuracy in estimating channel conditions. Also due to the time varying conditions of the channel, a delay between the time when the channel is estimated at the receiver and the time when the channel state information reaches the transmitter exists, and so the transmitter gets outdated channel information as the channel has already changed from what was predicted at the receiver.

2.9.1 Effect of Imperfect Channel State Information on Channel Capacity

Let us analytically analyze the approximate channel capacity in the case of imperfect channel state information at the transmitter. Optimal power distribution (which maximizes the channel capacity) for a time varying channel with AWGN is given by [16],

$$P(f) = \begin{cases} K - \dfrac{N_o(f)}{|H(f)|^2}, & f \in B \\ 0, & f \notin B \end{cases}, \tag{2.1}$$

where, *P(f)* is the power spectral density of the signal, N_o is twice the noise power spectral density, H(f) is the frequency response of the channel with total bandwidth B and K is a constant which determines the total power to be allocated. When we consider a non-ideal, bandlimited channel with AWGN, subdivided into N subchannels, each with

small enough bandwidth Δf such that the channel response is approximately constant within a subchannel, then, the channel capacity is approximated as,

$$C \cong \Delta f \sum_{i=1}^{N} \log_2 \left[1 + \frac{P_i |H_i|^2}{N_{oi}} \right], \tag{2.2}$$

where P_i, H_i and N_{oi} are the signal power, channel frequency response and noise power for the ith subcarrier respectively. Using the power distribution of (2.1), the capacity would be maximized, yielding,

$$C \cong \Delta f \sum_{i=1}^{N} \log_2 \left[\max \left(\frac{K |H_i|^2}{N_{oi}}, 1 \right) \right]. \tag{2.3}$$

Now, from [14], if instead of the actual optimal distribution of power as given by (2.1), based on $N_{oi} / |H_i|^2$, we use the estimate distribution of power, $\hat{N}_{oi} / |\hat{H}_i|^2$, the resulting channel capacity would be,

$$\hat{C} \cong \Delta f \sum_{i=1}^{N} \log_2 \left[1 + \max \left(K - \frac{N_{oi}}{|\hat{H}_i|^2}, 0 \right) \frac{|H_i|^2}{N_{oi}} \right]. \tag{2.4}$$

Using (2.4) we can numerically calculate the capacity for some imperfectly known channel transfer function $\hat{H}$ (assuming N_{oi} is constant with respect to i, i.e., white noise) and thus gain an indication of the impact of the use of imperfect channel information in the distribution of power [17], [18]. Figure 2.7 shows the results of the numerical calculations of (2.3) and (2.4), normalized by frequency, for simulated frequency selective channels with a maximum delay of $10\,\mu s$. A useful measure of the channel variation is the product of the Doppler spread, f_d, and the feedback delay, τ_d. Four different values of the doppler-delay product, $f_d \tau_d$ are considered. It is seen that the performance degradation is negligible for $f_d \tau_d \leq 0.01$ but as the product $f_d \tau_d$ increases the performance degradation increases rapidly. [10, 19] studied the effect of noise on the

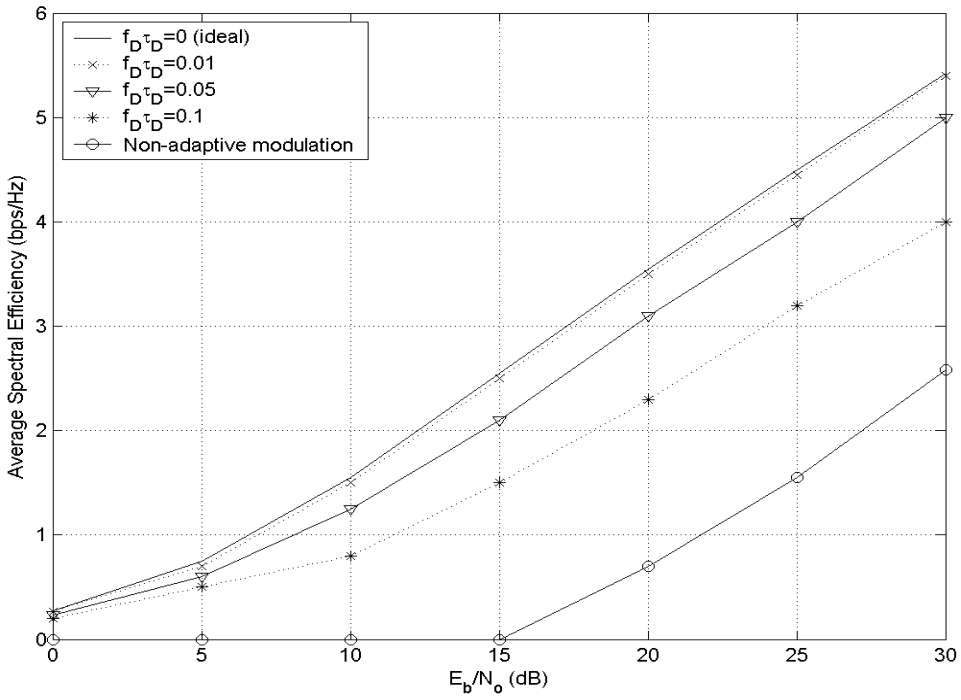

Figure 2.7 Average spectral efficiency of adaptive OFDM for various values of $f_d \tau_d$ due to delay in adapting CSI to the next block.

channel estimator. The channel estimator error is measured using the mean square error, which is defined below.

$$MSE = E\left\{\frac{1}{N}\sum_{i=1}^{N}\left|\hat{H}[n,i]-H[n,i]\right|^2\right\}, \tag{2.5}$$

where, $H[n,i]$ is the actual channel experienced by the ith subcarrier in the nth OFDM block and $\hat{H}[n.i]$ is the estimated channel. The estimated noise is characterized as AWGN such that $\hat{H}[n,i] = H[n,i] + e[n,i]$ where $e[n,i]$ is the estimator error, which is a complex Gaussian random variable with zero mean and variance σ_e^2 equal to the mean square error in (2.5). It has been shown in [17] that a performance loss less than -15 dB is tolerable and would not cause a significant problem in the applications of adaptive modulation.

2.9.2 Effect of Imperfect Channel State Information on the Performance of Adaptive OFDM

As the noise in the channel estimation causes minimal deterioration, we have studied the BER performance of adaptive OFDM with channel mismatch caused by the delay between the time when the channel is estimated at the receiver and the time when the transmitter adapts to that estimation information. The total bandwidth of 20 MHz is divided into 64 subcarriers, resulting in a block length of 3.2 μs . The carrier frequency is 5GHz and the maximum delay spread considered is 0.8 μs . The modulation levels were suitably adapted depending on the channel state information. BPSK, QPSK, 16-PSK and 64 PSK schemes were used and the overhead due to the guard interval was ignored. The bits were loaded onto the subcarriers in order to achieve a data rate of 5Mbps and to minimize the BER. The different loading algorithms are discussed in detail in the next chapter. Figure 2.8 shows the BER performance of adaptive OFDM in imperfect channel state information case.

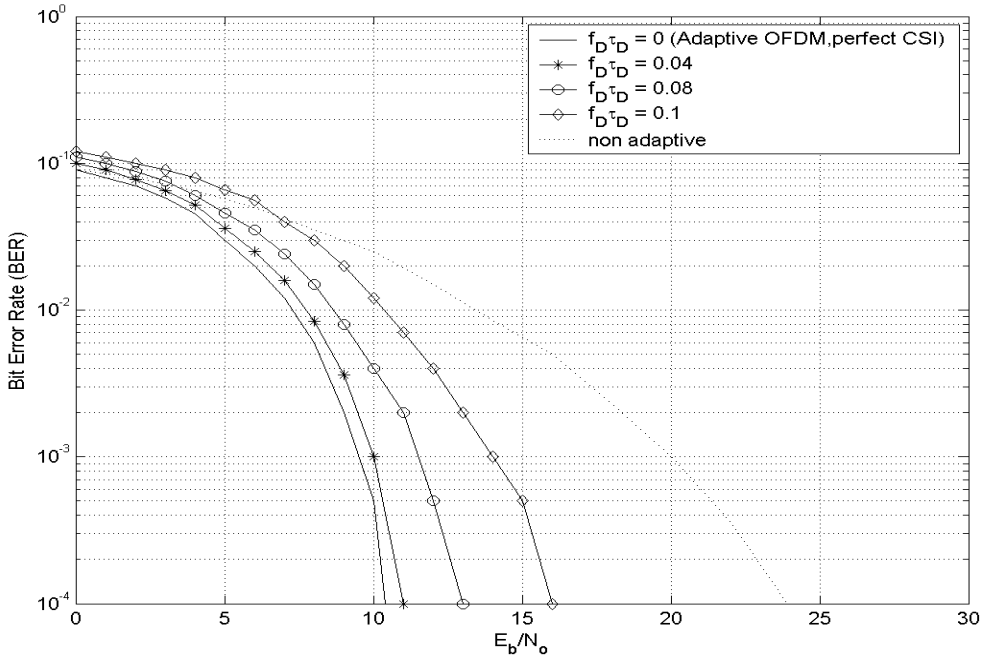

Figure 2.8 Performance of adaptive OFDM under imperfect channel state information due to delay in receiving the channel estimation.

The BER performance in case of non-adaptive OFDM and the performance in case of perfect channel state information are also shown for comparison purposes. We observe that when perfect channel state is available at the transmitter, a fair amount of gain in performance is possible as compared to non adaptive modulation. Also, as the doppler-delay product, $f_d \tau_d$, increases, more SNR is required in order to obtain the same level of BER. The results show that the performance degradation is severe at higher $f_d \tau_d$ product which is usually the case in outdoor wireless environments [20].

Summarizing, employing adaptive modulation with OFDM, whereby the bit, power and the probability of error are adapted to the channel state, has the potential to offer performance gains compared to fixed, uniform modulation. Even though Adaptive OFDM has limitations in case of imperfect channel conditions the performance gain is still significant in presence of channel estimation error, for relatively slowly varying channels. However, the impact of channel mismatch in the presence of quickly varying channels can be significant, as indicated by the capacity analysis and also verified by the BER simulations. Performance degrades as the delay in the channel estimation increases. Chapter 3 discusses the different methods to load bits on the subcarriers so to maximize the data rate, minimize the probability of error or to minimize the total power.

CHAPTER 3
ADAPTIVE BIT LOADING TECHNIQUES

3.1 Different Bit Loading Techniques

As we discussed in Chapter 2, for improving the performance of modulation techniques, the transmission strategy needs to be suitably adapted with the channel variation. This adaptation may include varying one or more parameters like the symbol rate, the transmission power, the constellation size, the coding rate/scheme. The goal of this adaptation is to increase link spectral efficiency (bps/Hz), lower BER, conserve transmit power, reduce interference to other users or meet various requirements of delay for different types of data [21], [22].

Several adaptive loading algorithms that exploit the efficient use of these parameters have been proposed. The question then arises as to which of these parameters should be adapted to obtain the best performance. It has been shown in [23] that adaptively varying one or two parameters achieves performance closer to the maximum possible spectral efficiency than that obtained by utilizing all the parameters. This chapter presents a systematic study of efficient loading of bits on the subcarriers by optimally varying one of the parameters among the data rate, power and the instantaneous BER. Note that we do not consider channel coding in this thesis. In this chapter, adaptive bit rate, adaptive BER and power adaptive techniques are studied.

3.1.1 Rate Adaptive Technique

In this technique, the total data rate is maximized while keeping constraints on the total power and the bit error rate. This can be mathematically described as,

$$\text{Maximizing the total data rate, b} = \max \left\{ \sum_{i=1}^{N} b_i \right\}, \tag{3.1}$$

where, N is the total number of subcarriers in an OFDM block and b_i is the data rate for the i^{th} subcarrier.The transmit power, P_o and total probability of error, BER, P_e are kept fixed and are given as,

$$P_o = \sum_{i=1}^{N} P_i \text{ and } P_e = \sum_{i=1}^{N} P_{ei}, \quad (3.2)$$

where, P_i is the power in and P_{ei} is the probability of bits in error in the i^{th} subcarrier.

3.1.2 Fixed Throughput Technique

As the name suggests, the data rate is kept constant along with the power and the total probability of error is minimized. It can be mathematically described as,

$$\text{Minimizing the total probability of error, } P_e = \min\left\{\sum_{i=1}^{N} P_{e^i}\right\}, \quad (3.3)$$

Where N is the number of carriers in an OFDM block and the bit rate, b, and the power are kept fixed in all OFDM blocks and are given as:

$$b = \sum_{i=1}^{N} b_i \text{ and } P_o = \sum_{i=1}^{N} P_i. \quad (3.4)$$

3.1.3 Power Adaptive Technique

This technique tries to minimize the total power subject to the constraint of maintaining a fixed rate and probability of error. It can be mathematically described as

$$\text{Minimizing the total power in each block, } P_o = \min\left\{\sum_{i=1}^{N} P_i\right\}, \quad (3.5)$$

where, N is the number of subcarriers and the data rate and power are kept constant in each OFDM block and are given as:

$$b = \sum_{i=1}^{N} b_i \text{ and } P_e = \sum_{i=1}^{N} P_{e^i}. \quad (3.6)$$

Let us now study each of these techniques in detail.

3.2 Rate Adaptive Technique

The goal of this adaptive loading algorithm is to increase the spectral efficiency by maximizing the data rate, keeping constraints on the power and probability of error. Bits are assigned on the subcarriers successively until the target rate R_T is reached. The

subchannel for which the transmission of an additional bit can be done meeting the constraints on power and the bit error rate is then selected. Note the denomination subchannel and subcarrier are used synonymously.

Chow *et all* [24] proposed an algorithm which optimizes the transmission bandwidth to maximize data rate under the constraint of power allocation and BER [25]. The total transmit power is equally distributed over subchannels, and bits are loaded onto the carriers with the strategy of using a large number of bits for subchannels with high gain, and using a small number of bits for subchannels with low gain. This algorithm is explained in detail below.

3.2.1 Chow Algorithm

It consists of three main sections. It first approximately finds the optimal system performance margin, γ_{margin} , which can be described as the additional amount of noise(in dB) that the system can tolerate while still trying to meet the minimum BER requirement. Then it iteratively loads bits on the carriers till the data rate is maximized, and lastly it adjusts the energy distribution accordingly on a subchannel by subchannel basis. Figure 3.1 shows the flow diagram representation of this algorithm.The mean SNR is first computed, the number of bits i.e. the modulation scheme are assigned in advance in accordance to the calculated SNR and the target probability of error. The system performance margin is assigned to zero, $\gamma_{\text{margin}} = 0$ (dB) and number of carriers is initialized to maximum, N. The number of bits on a subcarrier is calculated using,

$$b(i) = \log_2\left(1 + \frac{SNR(i)}{\Gamma + \gamma_{\text{margin}}(\text{dB})}\right) \tag{3.6}$$

$$\begin{aligned} \hat{b}(i) &= \text{round}[b(i)] \\ diff\,(i) &= b(i) - \hat{b}(i) \end{aligned} \tag{3.7}$$

where, Γ is, in effect, a tuning parameter known as the gap approximation. Different values of this parameter yield different number of bits to transmit which in turn allows us to characterize the BER performance of the system. $diff\,(i)$ gives the quantization error, as a result of loading integer number of bits on the subcarriers.

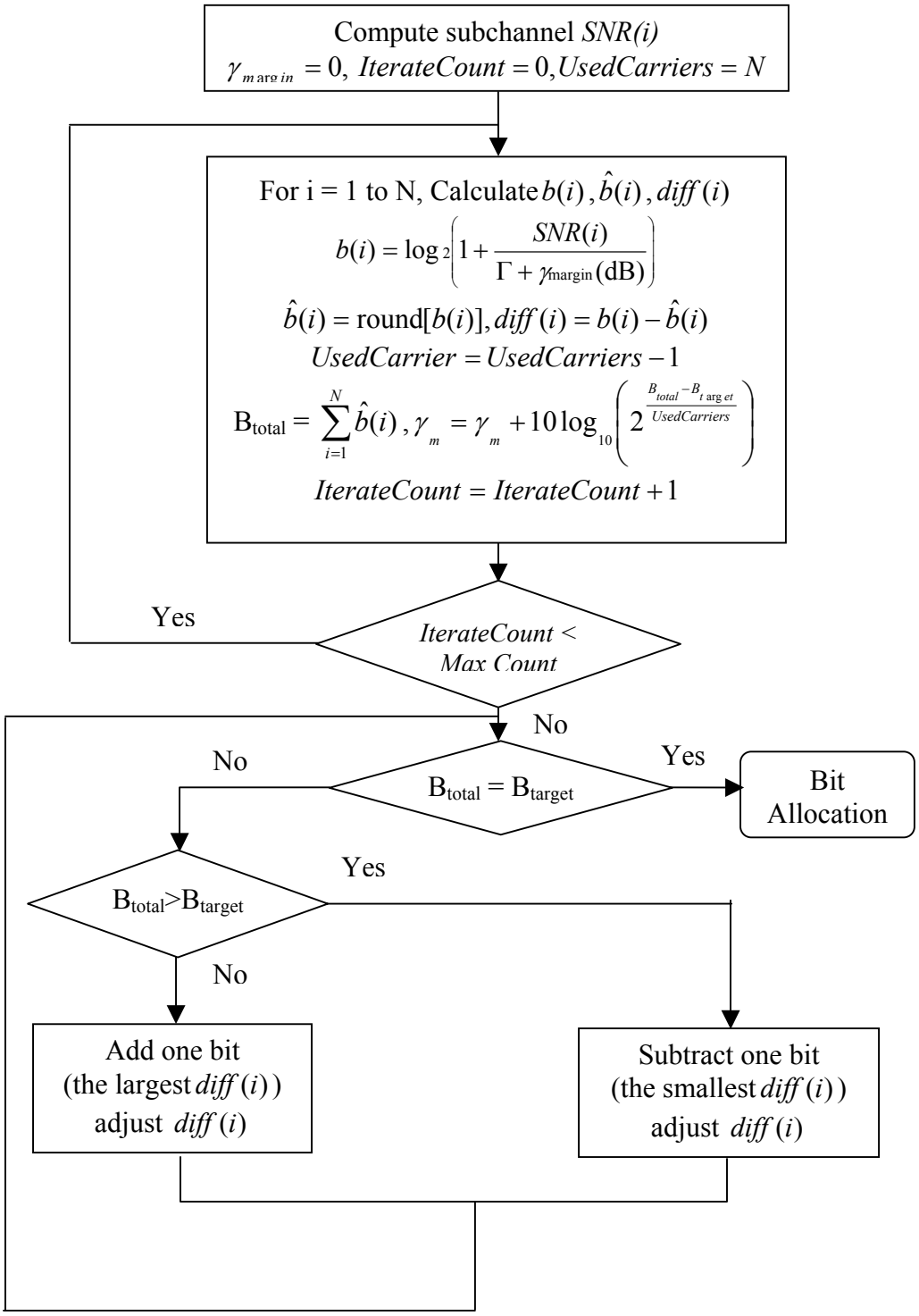

Figure 3.1 Flow diagram representation of Chow rate adaptive algorithm.

Until the total number of allocated bits equals the target total number of bits and the number of iterations is equal to the maximum count defined, it adds or subtracts one bit at a time from $\hat{b}(i)$ on the block of subcarriers. If $B_{total} = \sum_{i=1}^{N} \hat{b}(i)$ is less than B_{target} then one bit is added to $\hat{b}(i)$ on the carrier that has the largest diff (i) for that particular carrier. If B_{total} is greater than B_{target} then it subtracts one bit from $\hat{b}(i)$ on the carrier that has the smallest diff (i). This procedure is repeated until $B_{total}=B_{target}$. The transmit Power is allocated equally to all subcarriers i.e. $P_e(i) = P_{e,target} \ \forall i$ [24].

The advantage of this algorithm is that it converges fast but is computationally very complex and it quantizes the number of bits per carrier. During quantization in each subcarrier, the algorithm might decrease the bit rate resulting in loss in capacity.

[26] proposed a modification of Chow algorithm by allocating the same modulation scheme to adjacent subcarriers within one block. The spectral efficiency of a modulation scheme equals its average data rate, R per unit bandwidth, B. It is represented as, Spectral Efficiency $= \frac{R}{B}$ bits/second/Hz. The number of bits per symbol is $\log_2 M$ and the symbol time is T_s.

3.2.2 Mathematical Expression for Spectral Efficiency

The overall bit-error probability for all available modulation schemes in each OFDM block, taking into account the non constant SNR values γ_k across N_s subcarriers in the k^{th} block, is denoted by

$$\overline{p_e}(n) = 1/N_s \sum_k p_e(\gamma_k, M_n) . \tag{3.8}$$

In order to obtain the mathematical formula for optimal rate adaptation using different modulation techniques, we need an expression for its BER in AWGN for each technique. A closed form expression for Symbol Error Rate (SER) for MPSK as a function of SNR and constellation size as given in [16] is

$$P_s = 2Q\left(\sqrt{2g\frac{Eb}{No}}\sin\frac{\pi}{M}\right), \tag{3.9}$$

and the probability of bit error is given as,

$$P_e \approx \frac{1}{g} P_s \text{, where g = } \log_2 \text{M.} \tag{3.10}$$

But as we see that this equation is neither easily invertible nor easily differentiable in its arguments and using it to maximize the data rate is seemingly difficult. [23] found by curve fitting, an approximation to the above equation for Probability of bit error, P_e,

$$Pe \approx 0.25 \exp\left[\frac{-8g \frac{E_b}{N_o}}{2^{1..94g}} \right]. \tag{3.11}$$

Extending the above approximation to associate channel frequency response for the k^{th} subcarrier in the n^{th} block [n,k], to *Pe*, we get the instantaneous BER for the k^{th} subcarrier in the n^{th} block as,

$$Pe[n,k] = 0.25 \exp\left[\frac{-8 \frac{Es}{No} |H[n,k]|^2}{2^{1.94b[n,k]}} \right], \tag{3.12}$$

where, b[n,k] is the integer number of bits per symbol in the k^{th} subcarrier of the n^{th} OFDM block. E_s/N_o is the signal-to-noise ratio (SNR).

[17] used another variation of the Chow Algorithm. Bits are loaded on the carriers to achieve the target BER, P_{target} by setting the instantaneous BER, P_e[n,k] equal to P_{target}. So, we can find the number of bits transmitted in each subcarrier by inverting (3.12) above.

$$a[n,k] = \frac{1}{1.94} \log_2 \left[\frac{8\left(\frac{E_s}{N_o} \right) |H[n,k]|^2}{\ln\left(\frac{P_{target}}{0.25} \right)} \right]. \tag{3.13}$$

Also, the average spectral efficiency, S, can be given as,

$$S = E_{H[n,1],\ldots,H[n,N]}\left\{\frac{1}{N}\sum_{k=1}^{N} b[n,k]\right\}. \tag{3.14}$$

Because of identical statistics of H[n,k] for all values of k, we get the expression of spectral efficiency as,

$$S = E_{H[n,k]}\{a[n,k]\}. \tag{3.15}$$

Using this rate adaptive algorithm, the performance of adaptive modulation using different modulation schemes was evaluated. We have used Discrete Rate adaptation where only a discrete finite set of N constellations is available as compared to continuous rate adaptation where the set of signal constellations is unrestricted. The modulation levels used were BPSK, QPSK, 16PSK, 64PSK and the constraint on the probability of error was kept at 10^{-3}.A total bandwidth of 20 MHz is divided into 64 subchannels, resulting in a block length of 3.2 μs . The carrier frequency is 5 GHz. We assume that each subchannel in OFDM is narrow enough so that it experiences flat fading. The parameters are similar to those for IEEE 802.11a wireless local area networks [17]. Figure 3.2 shows the spectral efficiency of adaptive OFDM for the target BER of 10^{-3}.ICI and overhead due to the guard interval are not considered. The bits were loaded on the subcarriers using the Chow Algorithm as well as by using the formula [3.13, 17].As seen from the graph, the spectral efficiencies for the two different bit loading techniques under the same BER constraints are very close to each other. The throughput obtained when loading the bits using the derived formula is slightly less compared to when bits are loaded per the Algorithm. This is because the invertible formula is derived using curve-fitting techniques. This difference is almost negligible as compared to the complexity involved while using the Algorithm.

3.2.3 Fixed Threshold Algorithm

This algorithm overcomes the complexities of Chow Rate Adaptive Algorithm. It is based on defining the SNR thresholds [27], [28]. We can define the SNR threshold as

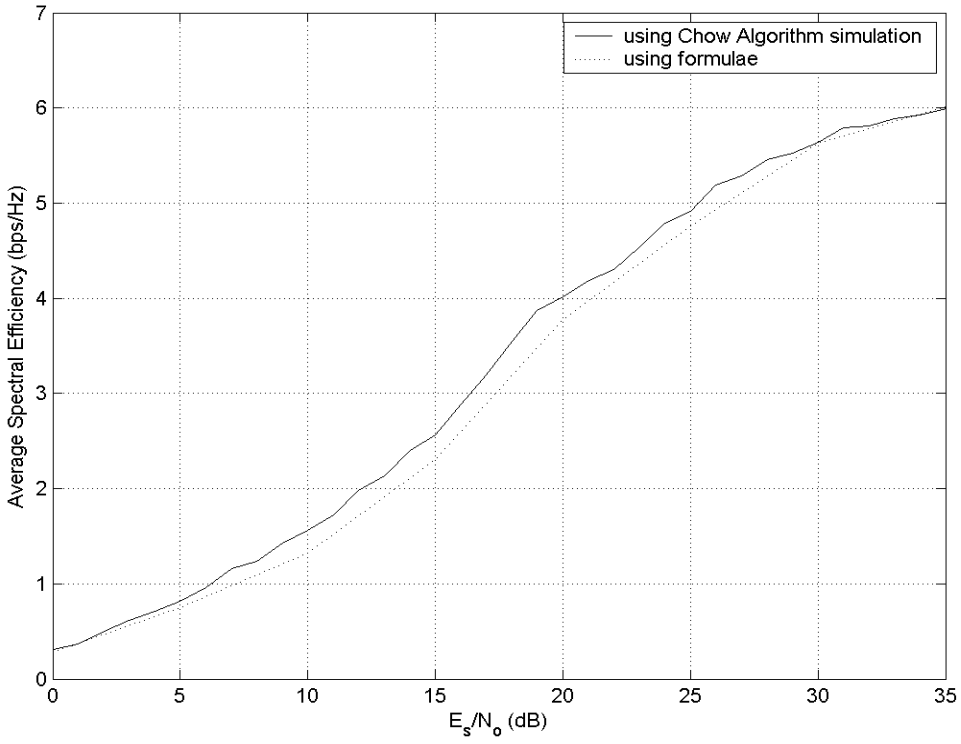

Figure 3.2 Average spectral efficiency for rate adaptive OFDM using the Chow algorithm and the mathematical formula (3.13 and 3.15).

the signal-to-noise ratio respectively for each modulation, above which that modulation is the most appropriate in terms of throughput. Thus if the instantaneous channel SNR exceeds the switching level l_n, modulation scheme M_n is selected. Mathematically, the rate region boundaries $\{\gamma_i\}_{i=0}^{N-1}$ define the range of SNR values over which different constellations are transmitted. Specifically, we assign one signal constellation and corresponding data rate of b_i bits/symbol to each rate region.$[\gamma_i, \gamma_{i+1}]$ $(0 \le i \le N-1)$, where, $\gamma_N = \infty$. When the instantaneous SNR γ falls within a given region, the associated signal constellation is transmitted. No signal is transmitted if $\gamma \le \gamma_0$.Thus, γ_0, serves as a cutoff SNR below which channel is not used. When the channel quality is significantly degraded, the channel should not be used. Figure 3.3 shows the flow diagram of the algorithm. This algorithm consists of the following steps.

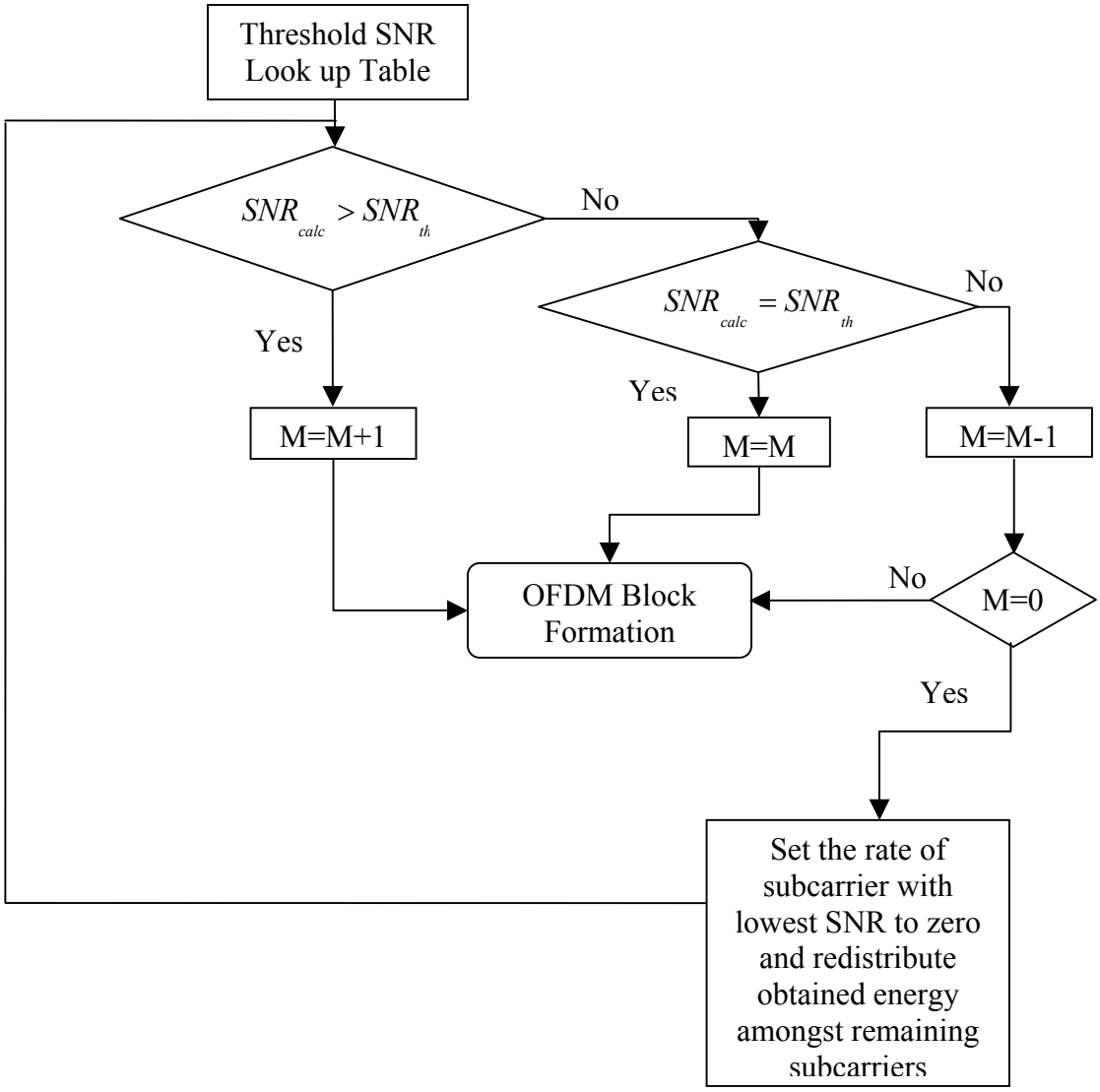

Figure 3.3 Flow diagram representation of fixed threshold algorithm.

The first step is the bit assignment and it assigns rate for each subcarrier by comparing current SNR of the subcarrier with the threshold for each modulation. The next step is the energy distribution. If for any subcarrier the assigned rate is zero, set the rate of the subcarrier with the lowest SNR to zero and redistribute the obtained energy amongst the remaining subcarriers and return to the first step. The algorithm terminates when all remaining subcarriers have non-zero rates [27], [28] and [29].

Following this flow diagram, this algorithm was implemented. Figure 3.4 shows the plot of the throughput versus SNR and it is also compared with the throughput obtained while using Chow's Algorithm. The throughput of the fixed threshold algorithm is heavily dependent on the SNR thresholds and these must be correctly chosen. They are chosen using an iterative approach till the desired throughput is achieved at the given constraints of transmitted power and BER as well as under the channel condition approximations in which the signal is going to be transmitted. At low SNR [0-5dB] the two algorithms perform the same but the fixed threshold algorithm out performs the Chow Algorithm at higher SNR. At 15dB SNR the fixed threshold algorithm sends bits with a spectral efficiency 0.5 bps/Hz greater than those sent using Chow Algorithm. 2dB power gain is achieved by using Fixed Threshold Algorithm when the average spectral efficiency is 2b/s.

The advantage of the fixed threshold algorithm lies in its simplicity and that it overcomes the quantization problem occurring in Chow Algorithm. Another advantage is that for different coding schemes, the same algorithm works just by altering the thresholds. The threshold values in Table 1 have been optimized for no coding. With coding the thresholds could be reduced. Using the idea from [30], the effect of various modulation scheme combinations on the spectral efficiency of OFDM was studied in the next section.

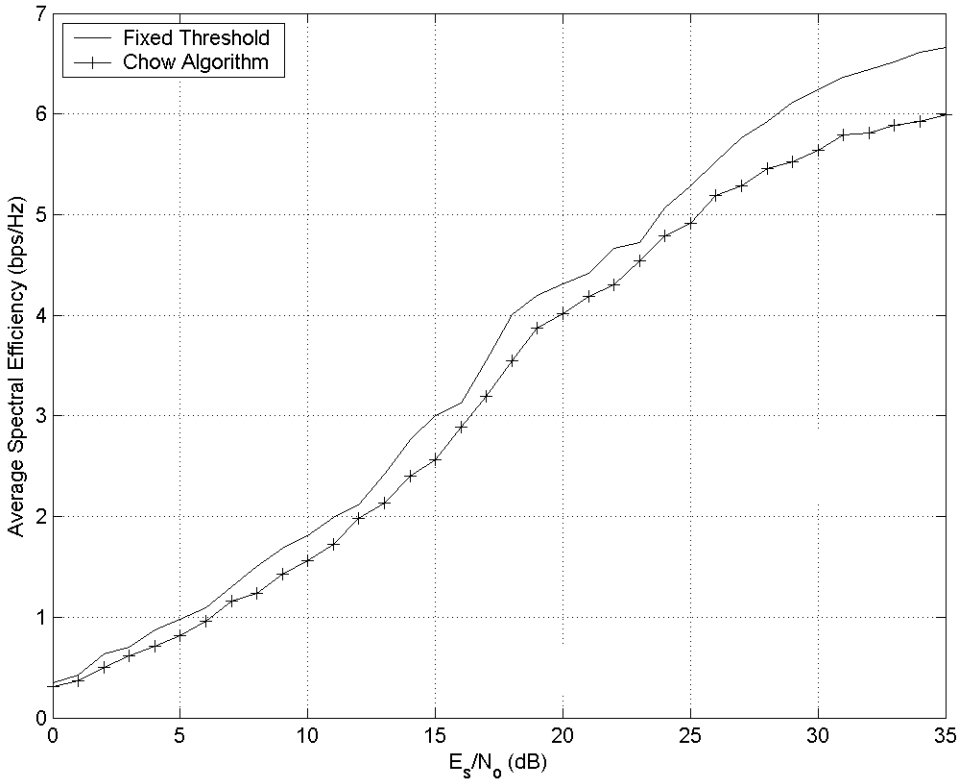

Figure 3.4 Comparing the average spectral efficiency of adaptive OFDM using Chow and fixed threshold algorithm.

Table 1 SNR Thresholds

Modulation	**SNR[dB]**
No transmission	SNR < 3.37
BPSK	SNR > 3.37
QPSK	SNR > 7.98
16PSK	SNR > 10.42
64PSK	SNR> 16.76

3.2.4 Effect of Various Modulation Scheme Combinations

The performance of fixed threshold algorithm using various modulation scheme combinations was evaluated. Different variations of modulation schemes were used to find the combinations which yields high spectral efficiency.

Case1: BPSK, QPSK, 16PSK and 64PSK

Case2: BPSK, QPSK, 16PSK

Case3: QPSK and 16PSK

The comparison was performed keeping the constraints on the probability of error, $P_{target} = 10^{-3}$.The SNR thresholds for the different modulation schemes were used from Table 1. From the simulation results plotted in Figure 3.5 we observe that the Case 1 achieves the best throughput performance as it suitably adapts the different modulation schemes based on the channel condition.

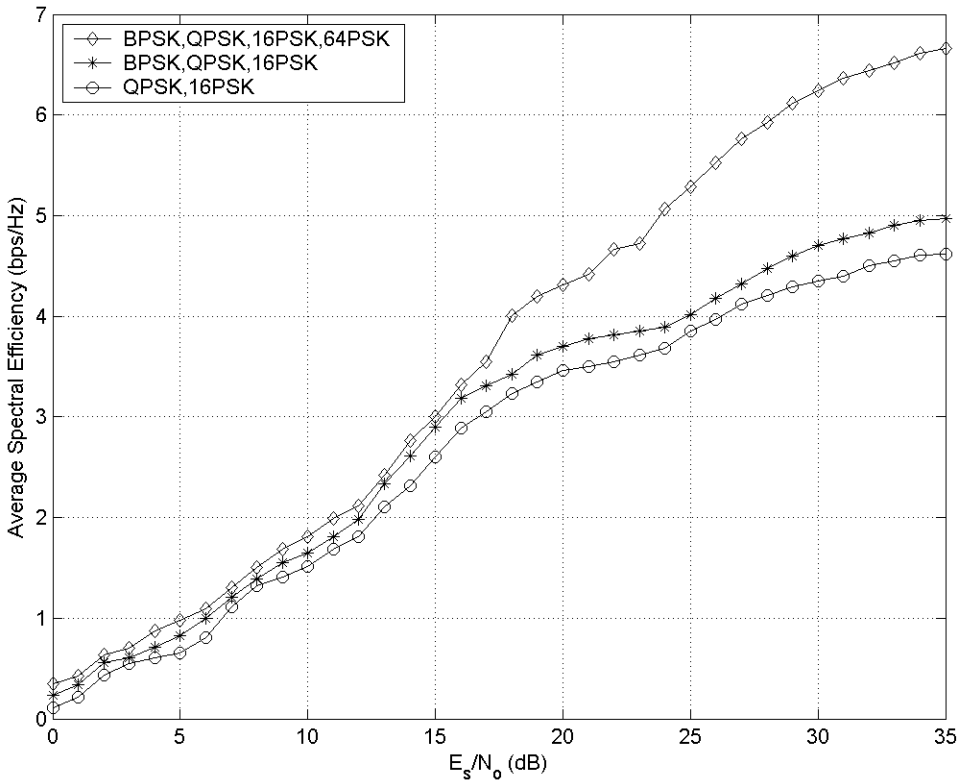

Figure 3.5 Average spectral efficiency of adaptive OFDM using various modulation level combinations.

In case of low SNR or poor channel condition fewer bits are transmitted using lower order modulation schemes and at higher SNR or in case of good channel condition high level modulation schemes like 16PSK and 64PSK are used and throughput performance increases. Also observed is that, at low SNR [0-17dB] the spectral efficiency of case 1 and 2 is the same as at lower SNR, lower level modulations are used. As case 2 doesn't use a higher-order scheme of 64PSK, we observe that the efficiency of case 2 drops when compared to case 1 after 17dB onwards. Case 3 gives the worst throughput performance as it doesn't use BPSK and 64PSK so it has a wide threshold SNR gap to switch the modulation scheme. So its efficiency suffers. Case 1 obtains an improvement of about 7dB more than case 3 at throughput performance of 4 bps/Hz.

3.2.5 Effect of Various Target BER's

The throughput performance was studied for different values of the target probability of error. We know that as the BER restrictions are reduced fewer bits are transmitted and spectral efficiency decreases. We have used 3 different BER restrictions of $1*10^{-3}$, $5*10^{-3}$ and $10*10^{-3}$. Figure 3.6 shows the graph of the average spectral efficiency versus signal-to-noise ratio with various target BER case. We observe that at low SNR, fewer bits are transmitted and the low BER case of 10^{-3} gives high throughput as it adapts suitably under those conditions and transmits bits using lower modulation schemes efficiently. As SNR increases [> 14 dB], we observe the general trend. At a given higher SNR, the throughput performance of higher BER [$10*10^{-3}$] is better, as it transmits more bits/second using higher modulation schemes and also the restriction on probability of error is lesser whereas for greater restrictions on the BER [$1*10^{-3}$ and $5*10^{-3}$], lesser bits/second are transmitted using the lower level schemes. So the case with BER=$10*10^{-3}$ achieves a gain of 6dB and 2dB over those with BER constraints of $1*10^{-3}$ and $5*10^{-3}$, at a throughput of 3 bps/Hz.

3.3 Fixed Throughput Technique

Wireless communication systems have to support a wide range of applications including voice, high-speed data, video, and image transmission. In general transmitting

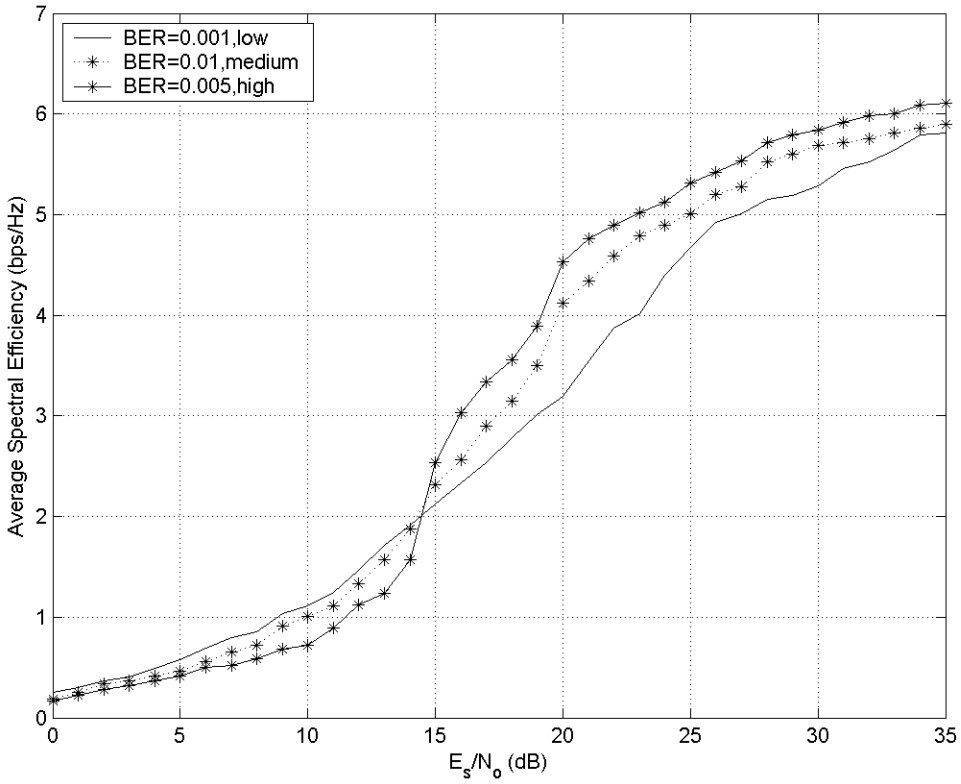

Figure 3.6 Average spectral efficiency for adaptive OFDM with P_{target} = [1, 5 and 10] $*10^{-3}$**.**

voice has low data rate requirements with real time delay constraints, while data transmission demands higher rates with less stringent delay requirements.

Thus to transmit voice we require fixed rate transmission. Also in military applications where one cannot afford losing important messages, we send the data at a fixed rate, keeping the error rate to minimum. This is achievable using a fixed throughput technique [22]. In this section we will study the fixed throughput technique in which the probability of error is minimized while keeping the total data rate and overall power constant. Each subcarrier is adaptive from block to block but the total power and the

number of bits remain fixed in every block. We will study to different algorithms to load the bits on the subcarriers and the total number of bits in a block is kept constant.

3.3.1 Cost Algorithm

The modulation schemes are assigned to the subcarriers using the cost function. This cost function is calculated based on the expected number of errors in each subcarrier. The expected number of bit errors, $e_{n,m}$ for each subcarrier, n and for each possible modulation scheme mode m, is calculated based to the estimated channel transfer function $\hat{H}$, as well as a function of the number of bits transmitted per subcarrier and modulation scheme, $b_{n,m}$.

Each subcarrier is assigned a state variable m_n holding the index of the modulation scheme and each state variable is initialized to m_0, the lowest order modulation scheme, which is for no transmission. A set of cost values are calculated for each subcarrier n and state m as follows,

$$c_{n,m} = \frac{e_{n,m+1} - e_{n,m}}{b_{n,m+1} - b_{n,m}}. \tag{3.16}$$

This cost value calculates the expected increase in the number of bit errors divided by the increase in throughput, if the next available modulation scheme is chosen. Thus, in other words it finds out the expected incremental increase in error if the transition to the higher modulation scheme were made.

The modulation scheme is found by iterative search for the block n having the lowest value of $c_{n,m}$ and incrementing its state its state m_n. This is repeated until the total number of bits in the OFDM symbol reaches the target number of bits. This algorithm allocates more bits to those subchannels with high frequency response and fewer bits or even no bits to subchannels with low frequency response values [27], [28] and [31].

The flow diagram in Figure 3.7 illustrates the steps involved in loading the bits on the subcarriers using the cost algorithm. The number of bits in an OFDM block is kept constant but the number of bits on the subcarriers in an OFDM block is adaptive. Following the above steps this algorithm was implemented and a system was simulated transmitting data at a fixed rate and constant power, minimizing the BER.

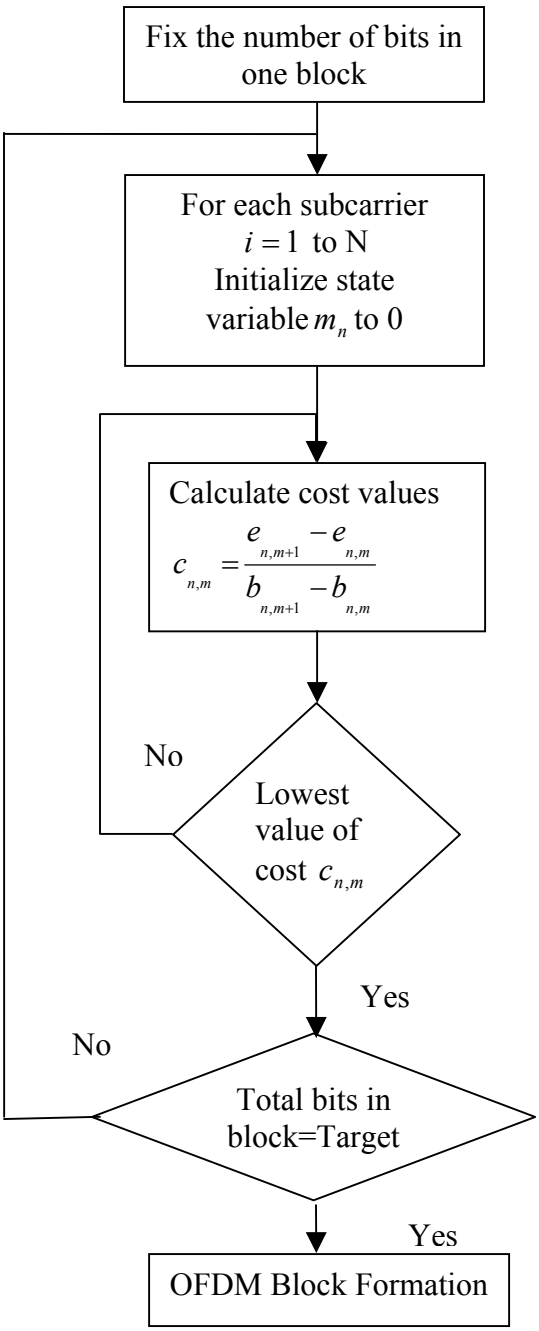

Figure 3.7 Flow diagram for loading bits on the subcarrier using the cost algorithm.

Figure 3.8 gives an overview of the BER performance of fixed throughput 64 subcarrier OFDM model for combinations of different modulation schemes. Different combinations of modulation levels were tried to find the one which gives a good BER performance.

Case 1: BPSK QPSK 16 QAM 64PSK

Case 2: BPSK QPSK 16 QAM

Case 3: QPSK 16 QAM 64 PSK

Case 4: QPSK 64 PSK .

From Figure 3.8 we observe that Case1 gives the best BER performance as the different modulation schemes are adapted according to the various channel conditions. Lower order modulation levels are used at low SNR and even in case when channel frequency response is low and it shifts to the higher order modulation levels at high SNR and when the channel response is good. Thus it minimizes the BER efficiently. Case 2 compared to Case 3 doesn't use higher order modulation scheme like 64PSK and uses BPSK, so it transmits fewer bits compared to Case 3 but there fewer errors and so its BER performance is better than case 3. Case 4 gives the worst BER performance since it cannot adapt to the channel conditions and it uses two levels of QPSK in case of lower SNR and poor channels and a high level 64PSK for higher SNR and good channels and so the number of errors increases and it gives a worst BER performance. Case 1 achieves a SNR gain of 2dB over Case 2 and 10dB over Case 4 at BER of 10^{-2}.

3.3.2 Blockwise Loading Algorithm (Modification of Fixed Threshold Algorithm)

Using this algorithm, data are transmitted at constrained rate and power. The algorithm consists of three steps:

Step1: SNR Threshold

This step is similar to the step of comparing SNR with a threshold in the fixed threshold algorithm. This step calculates the current SNR of the carriers and assigns the modulation scheme to each carrier based on the calculated SNR threshold. It doesn't send bits on the subcarriers with SNR less than the lowest SNR threshold.

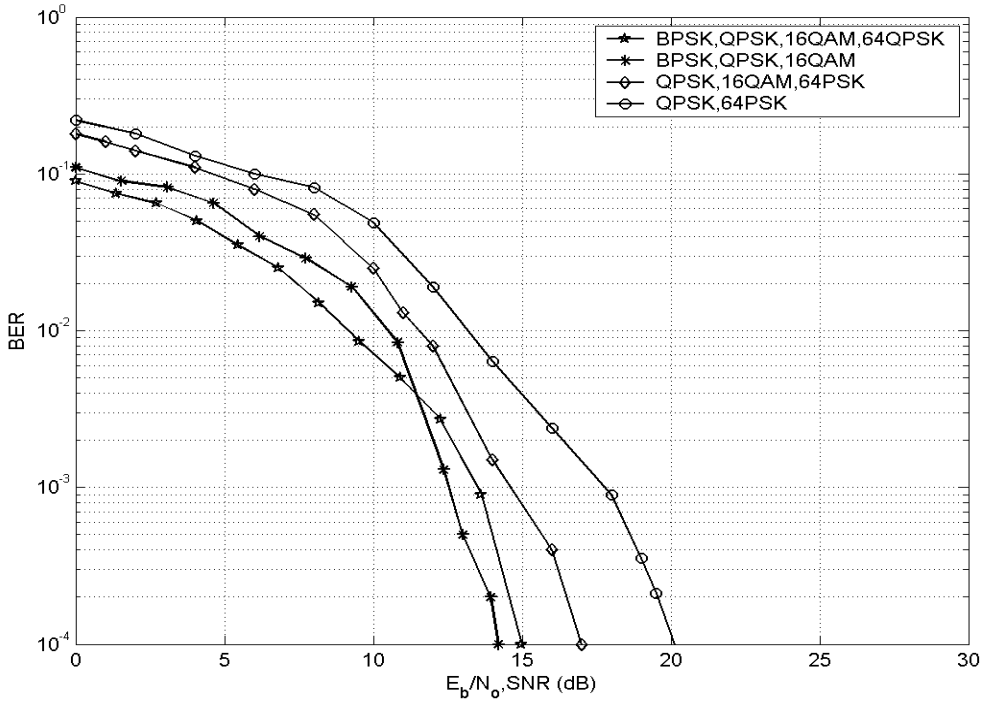

Figure 3.8 BER performance for fixed throughput adaptive OFDM using various modulation level combinations.

The available modulation schemes are BPSK, QPSK, 16PSK, 64PSK and the SNR thresholds are used from the Table 1.

Step2: Bit Tightening.

Here the algorithm modifies the schemes of subcarriers in order to reach the target rate. If the achieved rate in step 1 is lower than the target rate, the algorithm finds subcarrier whose SNR is closest to the upper threshold. When it is feasible the rate of this subcarrier is shifted to the next higher rate. This procedure is iterated until the achieved rate equals the target rate. If the achieved rate in step1 is higher than the target rate, the algorithm finds the carrier whose SNR is closest to the lower threshold. When it is feasible the rate of this subcarrier is shifted to the next lower rate. This procedure is iterated until the achieved rate equals the target rate.

Step 3: Power Balancing

At the end of bit tightening, some subcarriers have no data bits sent on them since they have experienced low SNR. The surplus power obtained from these subcarriers is distributed amongst the active subcarriers. This maintains the total power in each OFDM symbol at a constant value.

The flow diagram in Figure 3.9 illustrates this algorithm and, following the steps the subcarriers in a block are made adaptive but the number of bits in each block is fixed. The graph in Figure 3.10 gives an overview of the BER performance of the fixed throughput technique for a range of target bit numbers. The modulation levels used are BPSK, QPSK, 16PSK and 64 PSK. The target rates were varied from 1.5 bps to 6.5 bps and the BER was reviewed. The graph without markers represents the low data rate which transmits 1.5bps/Hz.It can be seen that as the data rate increases the BER performance decreases because in order to keep up with the data rate bits are loaded on the subcarriers using higher modulation schemes resulting in more errors and a poor BER performance. The SNR gain for a BER of 10^{-2} is 2dB compared to when the data rate is 2.5bps and 7dB and 8.5dB when the data rate is 4.5 bps and 6.5 bps respectively. Reducing the throughput by one third, 4.5 bps to 1.5 bps, the required SNR is reduced by 7dB for a BER of 10^{-2}, while increasing the throughput from 4.5 bps to 5.5 bps deteriorates the noise resilience by 1.5 dB at the same BER.

3.4 Adaptive Power Technique

The Adaptive Power Technique aims to minimize the transmitted power while providing a fixed rate and BER level. In [32], Huges-Hartogs developed a loading technique to minimize the transmitted power consumption under the requirements of data rate and BER. As the power needed to transmit a certain number of bits in a subcarrier is to be minimized, a greedy approach is used. It assigns one bit at a time to subcarriers, this method is known as successive bit allocation. In each assignment, the subcarrier that requires the least additional power is selected. The bit allocation process is completed when all the required bits are assigned. The approach presented in [32] was very complex. Several papers have provided various modifications to this algorithm to reduce

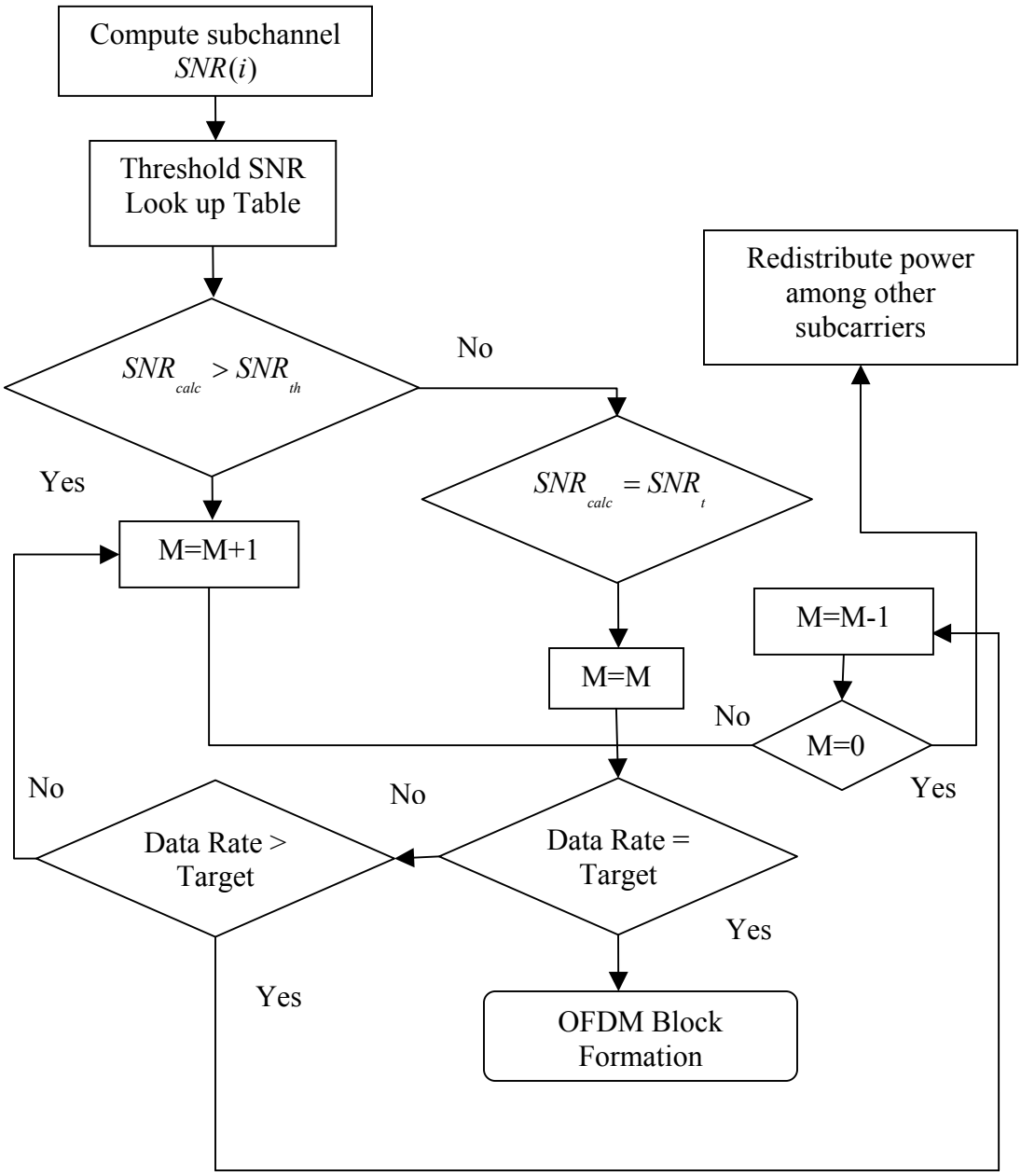

Figure 3.9 Flow diagram of blockwise loading algorithm.

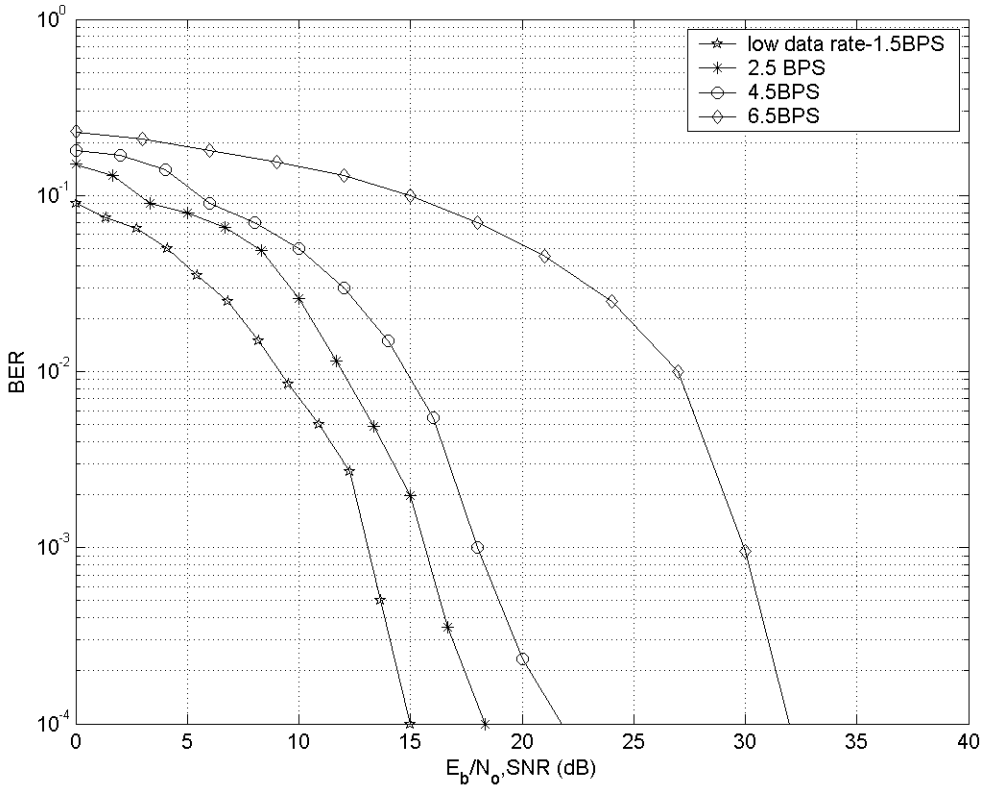

Figure 3.10 BER performance of adaptive OFDM using fixed throughput technique.

the complexity [33]. The basic structure of most algorithms is similar and described below. In the first step, the signal-to-noise ratios for the subcarriers are computed and the number of bits on the i^{th} subcarriers is assigned by,

$$b(i) = \log_2\left(1 + \frac{SNR}{\Gamma}\right). \tag{3.17}$$

where, Γ is the GAP Approximation. It is in effect a tuning parameter. Different values of this parameter yield different number of bits to transmit which allows us to characterize the BER performance of the system.

The number of bits *b(i)* are then rounded to take integer values 0,1,2,4,8 corresponding to no data, BPSK, QPSK, 16PSK, 64PSK modulation levels respectively.

The energy for the i^{th} subcarrier based on the number of bits assigned initially is computed using,

$$e_i(b(i)) = \frac{2^{b(i)} - 1}{SNR(i)/\Gamma}. \tag{3.18}$$

A table of energy increments is computed for each subchannel, which contains the additional power needed by the subcarrier to transmit an additional bit.

$$\Delta e_i(b) = e_i(b+1) - e_i(b) = \frac{2^{b-1}}{SNR/\Gamma}. \tag{3.19}$$

Bit Tightening is the next step and the energy increment table computed in the first step is made use in this step to optimize the bit allocation. If the constraint on the data rate is not satisfied by the initial bit allocation,

$$\sum_{i=1}^{N} b_i = R \tag{3.20}$$

and the rate obtained is less than the desired than the subcarrier that needs the minimum additional power is assigned one more bit and the new additional power for that subcarrier is updated. This procedure is repeated until the data rate is satisfied [34]. The flow diagram in Figure 3.11 illustrates the steps involved in loading the bits on the subcarriers minimizing the transmission power subject to rate and BER techniques. Figure 3.12 gives an overview of the BER performance of the power adaptive technique. The two set of solid line curves in the figure correspond to power adaptive technique's BER performance at a target BER's of 10^{-1} and 10^{-2} respectively. The modulation levels used are BPSK, QPSK, 16PSK and 64 PSK. The data rate is fixed at 1.5bps/Hz.The dotted line in the figure shows the plot of the BER performance of rate adaptive technique using the same modulation level combination as mentioned above. It is plotted side by side with the solid line curve to compare the BER performance of the two bit loading techniques with the same BER constraint levels and using the same combination of modulation levels. It is plotted side by side with the solid line curve to compare the BER performance of the two bit loading techniques using the same combination of modulation levels and with the same BER constraint levels. We see that the two techniques meet the BER constraints well but the BER performance of power adaptive

technique is better than the rate adaptive technique. This is because the rate adaptive technique tries to maximize the rate by using higher order modulation levels and so it has

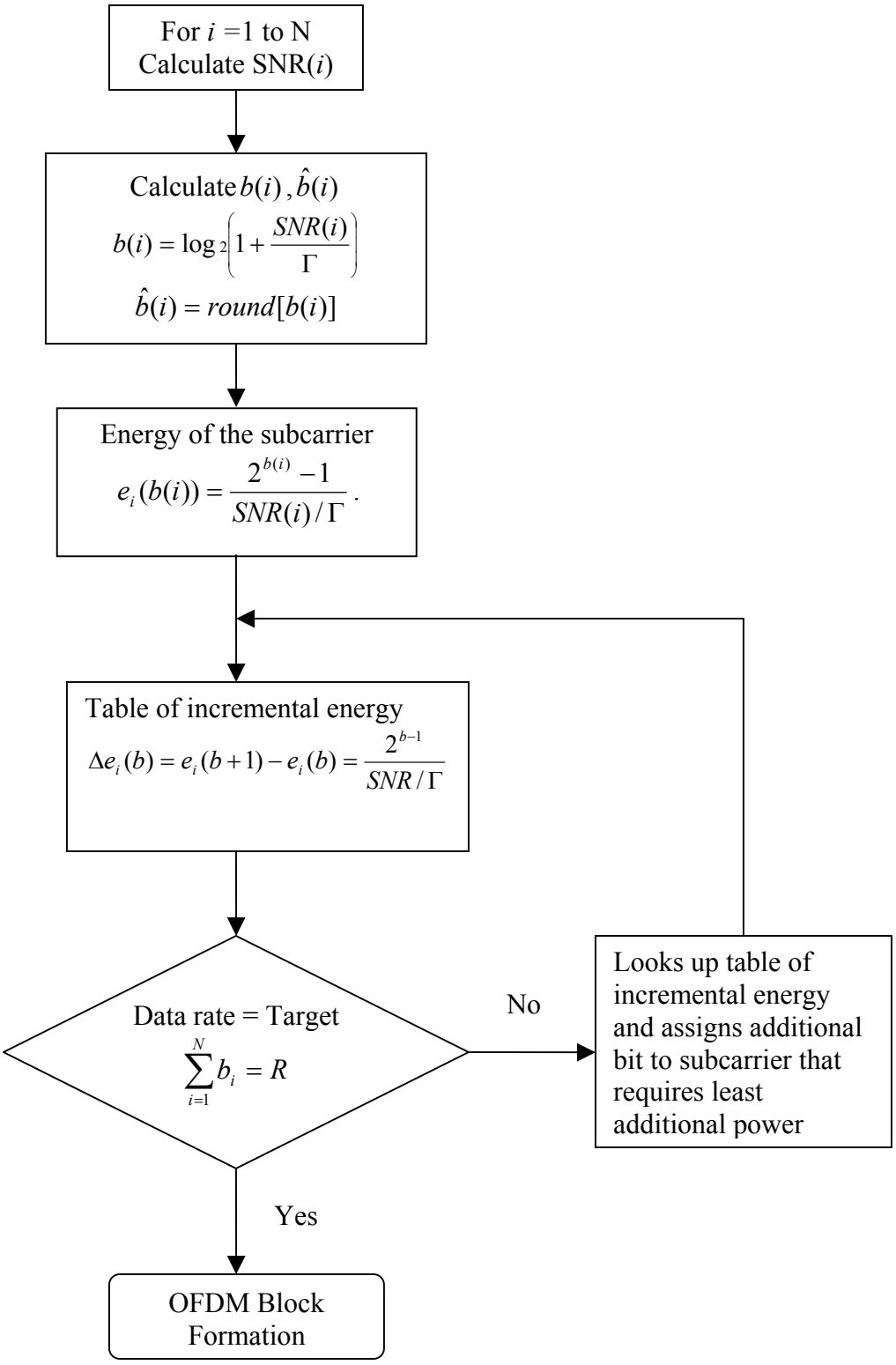
For i =1 to N
Calculate SNR(i)
Calculate $b(i)$, $\hat{b}(i)$
$b(i) = \log_2\left(1 + \frac{SNR(i)}{\Gamma}\right)$
$\hat{b}(i) = round[b(i)]$
Energy of the subcarrier
$e_i(b(i)) = \frac{2^{b(i)} - 1}{SNR(i)/\Gamma}$.
Table of incremental energy
$\Delta e_i(b) = e_i(b+1) - e_i(b) = \frac{2^{b-1}}{SNR/\Gamma}$
Data rate = Target
$\sum_{i=1}^{N} b_i = R$
No
Looks up table of incremental energy and assigns additional bit to subcarrier that requires least additional power
Yes
OFDM Block Formation

Figure 3.11 Flow diagram of adaptive power algorithm.

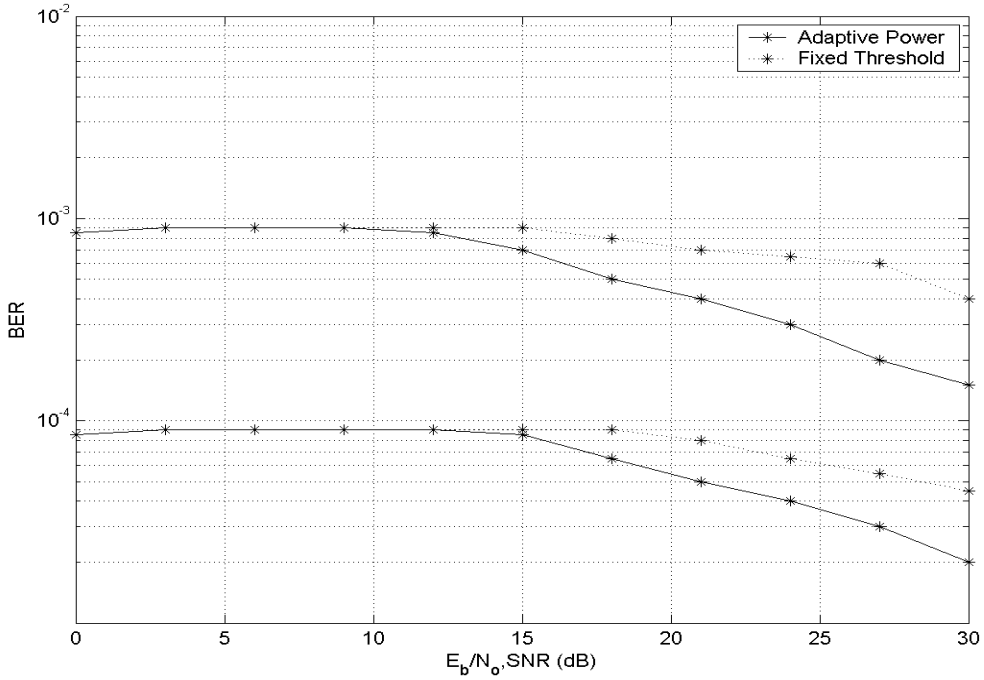

Figure 3.12 BER performance comparison of adaptive power and fixed throughput technique.

a higher error rate. The power adaptive technique has a constraint on the data rate, so at large SNR it has a control on the number of bits loaded and hence on the number of erroneous bits and so a better BER performance. It is also seen from the figure, as the BER constraint increases, the BER performance begins to improve at a higher SNR.

3.4 Comparison and Overview

We have thus studied the adaptive techniques with one degree of freedom, i.e. one parameter is varied subject to the constraints on the other two. In [35] both the data rate and the transmit power were adapted and it is shown that varying both the rate and the power leads to a negligible higher spectral efficiency over varying the data rate alone. Therefore using just one or two degrees of freedom in adaptive modulation yields spectral efficiency close to that obtained by using all degrees of freedom.

Also seen is that, of the three adaptive techniques discussed, the maximum spectral efficiency is achieved by the rate adaptive technique. This is because the rate adaptive technique allocates the rate adaptively across subchannels whereas the fixed throughput and power adaptive techniques have to provide an equal rate for all subchannels regardless of channel statistics.

Also observed is that the BER performance is much better when the rate is constrained and the power or the probability of error is minimized. The fixed throughput technique minimizes the probability of error and offers good BER performance. With adaptive rate technique, the constraint on BER is met well, but it gives a poor BER performance when compared with adaptive power technique.

Based on the computational complexity we have seen that the Chow rate distribution algorithm distributes rate based on the channel capacity of the subcarriers and requires sorting of the channel power gains at the transmission bandwidth identification stage, it is computational very complex and operation order is high. Whereas, the fixed threshold algorithm uses a lookup table method with precomputed rate SNR tables and so this algorithm requires a large memory to keep all values of operating points on rate-SNR curve. With the power adaptive algorithm extensive sorting is required and one bit is added at a time on subcarriers so the order of operations is expected to be- $O(\hat{B} * N * \log_2 N)$, where $\hat{B}$ denotes the total number of loaded bits and N is the number of subcarriers. Thus the complexity of different algorithms is different and the parameters to be adapted are chosen based on the implementation considerations.

The choice of the bit loading technique is application specific. For high speed data transmission, maximum spectral efficiency is desired at constrained BER, so rate adaptive technique is chosen. For voice transmission fixed-rate transmission is used, in situations where the error rate has to be kept minimum, fixed throughput technique is used and in others fixed rate transmission is combined with power adaptation, where the transmitter adjusts its power to maintain a constant SNR at the receiver.

Summing up, the adaptive techniques help improve the overall performance of the OFDM systems and the bit loading technique should be chosen depending on the application. Further work on this front is currently being carried on where the coding

schemes are used along with the adaptive techniques [36], [37] with imperfect channel conditions for different communication systems and better performance is achieved [38] and [39].

CHAPTER 4
PEAK TO AVERAGE POWER REDUCTION RATIO

4.1 Introduction

In previous chapters we have seen the usefulness of using adaptive OFDM against dispersion in multipath fading. Unfortunately, there are a number of disadvantages with implementing OFDM. One particular problem with OFDM is its large envelope fluctuation. When the sinusoidal signals of the N subcarriers add constructively, spurious high amplitude peaks in the composite time signal occurs. Compared to the average signal power the instantaneous power of these peaks is high. This is usually quantified by the parameter called Peak to average Power Ratio (PAPR) [40]. Since most practical transmission systems are peak power limited, designing the system to operate in a perfectly linear region often involves using power amplifiers at power levels below the maximum power available. This technique is not power efficient and causes high battery demand in mobile applications. Power efficiency is necessary in wireless communication as it provides adequate area coverage, saves power consumption, and allows smaller size terminals [41], [42]. The allocation of the radio spectrum limits the isotropically radiated peak envelope power. If the output peak is clipped, this generates out of band radiation due to intermodulation distortion. The first difficulty listed above is infact the cause of the second and third. These issues limit the usefulness of OFDM for some applications. Therefore, techniques to prevent the occurrence of such interference by controlling the PAPR of the transmitted signal with some manipulations to the OFDM signal itself are invaluable [43]. Although OFDM dates back to 1971, the existence of the PAPR problem was not recognized until 1994 [44]. Therefore, the literature on the PAPR-reduction problem is relatively recent, but given the importance of the problem, it has been extremely prolific. We will focus on the PAPR reduction techniques in this chapter.

4.2 Peak and Average Power Analysis of Modulated Signals

Digital vector modulated schemes that modulate a signal's amplitude (such as QAM), have multiple symbol power levels. Vectorial analysis of a signal's I-Q diagram

will reveal these levels. Since each symbol power level represents multiple symbol states, any system non linearities that could alter one of the symbol power levels (such as AM distortions) would also affect the system symbol error rate (SER). Impairments of this type would easily generate high SER which would disable an entire system [45]. Assuming that all symbol states are occupied equally over time; it is then possible to calculate the peak to average symbol power. Figure 4.1 below shows the calculation of peak to average symbol power and for QAM signal. PSK modulations have only one symbol power but are still vulnerable to amplifier nonlinearity distortions. Baseband filtering will introduce an additional peak power contribution in the form of compound amplitude ringing. A digital transition causes an impulse response that has an infinite Fourier series. Convolution of this series with a bandwidth limiting filter results in truncation of the series and also ringing or Gibbs Phenomenon. The amplitude of ringing will vary from symbol to symbol because certain phase/amplitude changes will be more drastic than others. This effect of symbols randomly transitioning across multiple power levels combined with the compound ringing from baseband filters will produce a complex power envelope that is continuously changing.

As said before, the highest (peak) power levels of this signal must be preserved within the linear region of the amplifier. Failure to do this will cause significant intermodulation distortions and if severe enough, a significant data loss. Because of these reasons QAM signals are often operated with average power levels 9 to 15 dB below a power amplifier's saturation level. PSK amplifiers usually require at least 7 to 10 dB of output back off as well. Transmitters that support multicarrier operations (multiple simultaneous carriers, OFDM) are further challenged due to the peak power effect that results from the vectorial addition of the voltage waveforms of each individual carrier. As seen from Table 2, each time the number of carriers (with equal power) in a system are doubled, the peak to average power ratio will increase by 3dB.In an example situation of 32-10W carriers, each being QPSK modulated, and having peak to average power ratios of 3dB (caused by baseband filter ringing), the combined average power would be 320 W (55 dBm), but because the total peak-to-average power ratio would be 21 dB (Table 3); the peak power could reach to almost 40,000 Watts. If the power amplifier were rated for

Symbol Power Level	Power Vector Magnitude	Number Of Occurrences	Weighted Symbol Power
1	1	4	4
2	5	8	40
3	9	4	36
Total weighted symbol power:			80
Divided by total number of symbol states:			16
Average symbol power magnitude:			5
Peak symbol power magnitude:			9
Peak/Average Power Ratio = 9/5 = 1.80 = 2.55 dB			
Dynamic Range = 9/1 = 9.54 dB			

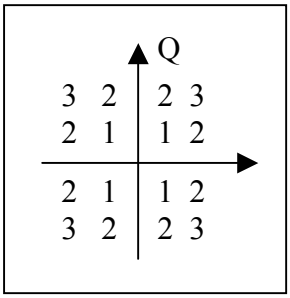

16-QAM

Type of Vector Modulation	Number of Symbol Power Levels	Peak to Average Power Ratio		Dynamic Range Ratio	
		Ratio	dB	Ratio	dB
16 QAM	3	1.8:1	2.55	9:1	9.54
32 QAM	5	1.7:1	2.30	17:1	12.31
64 QAM	9	2.3:1	3.68	49:1	16.90
256 QAM	30	1.9:1	2.85	157:1	21.96

Figure 4.1 Calculation of symbol power for QAM.

Table 2 Peak power contribution of multiple carriers

Number of Carriers (N) (1W each)	Average Power (P_{avg})		Peak Power ($P_{pk} = N*P_{avg}$)		Peak to Average Power Contribution	
	Watts	dBm	Watts	dBm	Ratio	dB
1	1	30	1	30	1:1	0
2	2	33	4	36	2:1	3
4	4	36	16	42	4:1	6
8	8	39	64	48	8:1	9

32	32	45	1024	60	32:1	15
64	64	48	4096	66	64:1	18

Table 3 Peak/Average power for 32 channel QPSK.

Peak Power Contribution:	32 channel QPSK
Peak/Average Symbol Power	0 dB
Baseband filter ringing	3.0dB
Multiple carrier addition	15.0dB
Sinusoidal cresting factor	3.0dB
Total Peak to Average Power	21.0dB

linear operation to 5 kW, since the peak to average power demand could not be supported, all peak power occurrences greater than 5 kW would drive the amplifier into a compression and saturation state.

Having understood the peak power effects in OFDM signals we can now mathematically define the PAPR for an OFDM signal. From [46], [47] and [48], a complex baseband OFDM symbol, defined over the time interval $t \in [0, T_s]$, can be expressed as,

$$s(t) = \frac{1}{\sqrt{N}} \sum_{n=0}^{N-1} A_n e^{j2\pi fct} \quad , 0 \le t \le T_s . \tag{4.1}$$

The N subcarriers are chosen to be orthogonal, that is,

$$f_n = n\Delta f = n / T_s , \tag{4.2}$$

where, A_n is the data for the n[th] subcarrier and T_s is the symbol duration. The peak to average power ratio (PAPR) of the baseband OFDM signals, *P* can be defined as

$$P = \frac{\max \ 0 \le t \le T_s |s(t)|^2}{P_{av}}, \tag{4.3}$$

where,

$$P_{av} = E[|s(t)|^2 = \sigma^2, \tag{4.4}$$

since A_n is assumed to be statistically independent, identically distributed random variable with zero mean and variance σ^2.We also alternatively consider the crest factor (CF) *C*, which is the square root of PAPR, i.e.,

$$C = \sqrt{P} = \max\ 0 \le t \le T_s \frac{|s(t)|}{\sqrt{P_{av}}} \tag{4.5}$$

In this thesis, we have not considered pulse shaping of the signals and the power spectral density of OFDM signal is approximated to be rectangular. The amplitude of OFDM signals can be written as,

$$|s(t)| = \left| R\left\{ s(t) e^{j 2\pi f_c t} \right\} \right|, \tag{4.6}$$

where, f_c is the carrier frequency. Since $f_c >> 1/T_s$, the peak power of the signals maybe equivalent to that of the complex baseband signals. Therefore, in what follows, we only consider the PAPR of baseband OFDM signals. From [41] had pulse shaping been considered, the maximum PAPR would be represented as

$$\text{PAPR}_{\max} = \frac{1}{N} \max\ 0 \le t \le T \left(\sum_{n=0}^{N-1} |p_m(t)| \right)^2, \tag{4.7}$$

where, $p_m(t)$ is a pulse shape of duration T_s used at subcarrier m,

$$\int_0^T \left| p_m(t) \right|^2 dt = T. \tag{4.8}$$

If the same pulse shape is used on every subcarrier, i.e.

$$p_0(t) = p_1(t) \ldots\ldots p_{N-1}(t) = p(t), \tag{4.9}$$

The maximum PAPR would be,

$$PAPR_{max} = N \max 0 \le t \le T_s \left| p_m(t) \right|^2 \quad (4.10)$$

Equation (4.10) indicates that smoothing the different subcarriers using the same pulse shape increases the PAPR of the transmitted signal. With such a structure the rectangular pulse gives the lowest PAR and appears to be the best choice.

Since we have assumed rectangular PSD of OFDM symbol, the maximum PAPR of the transmitted signal is lower bounded by

$$PAPR_{max} = N. \quad (4.11)$$

4.3 Clipping Technique to Reduce PAPR

Several solutions [49], [50] have been proposed to reduce the PAPR of the OFDM signal. One of the simplest technique is to deliberately clip the high amplitude OFDM peaks. Various clipping techniques have been described in literature [51].Some techniques limit the peak signals by clipping the output of the IDFT before filtering. But the signal must be filtered or interpolated before transmission and this leads to peak regrowth, so clipping before interpolation is not very effective in reducing the PAPR. To avoid this problem, the signal can be clipped after interpolation [52], [53]. Since clipping is a non linear process this causes inband distortion (BER) and out of band noise, which reduces the spectral efficiency.

If the samples are clipped at amplitude A then the n^{th} output sample can be represented as,

$$s_a = g(s_n) = \begin{cases} -A, s_n < -A \\ s_n, -A \le s_n \le A \\ A, s_n > A \end{cases}, \quad (4.12)$$

where, s_n is the n^{th} sample of the complex OFDM signal. The clipping ratio, CR is defined as the ratio of the clipping level to the square root of the mean power of the unclipped baseband signal.

$$CR = \frac{A}{\sqrt{P_{in}}}, \quad (4.13)$$

where, P_{in} is the input power of the OFDM signal before clipping. Since the amplitude s_n is a Rayleigh random variable with probability density function (pdf),

$$fs_n(s_n)\frac{2s_n}{P_{in}}e - s_n^2 / P_{in}. \tag{4.14}$$

The total output power P_{out}, is the sum of the signal and distortion components and is given by [48] as,

$$P_{out} = E_{rn}\left[g^2(s_n)\right] \tag{4.15}$$

$$= \int_0^\infty g^2(s_n) f_{s_n}(s_n) dr_n \tag{4.16}$$

$$= \left(1 - e^{-CR^2}\right)P_{in}. \tag{4.17}$$

Note that CR cannot be zero by definition of 4.13.However, considering the amplitude normalized by the rms output power, we may define CR=0 by its limit:

$$\lim_{CR\to 0} s_n \le \lim_{CR\to 0} \frac{A}{\sqrt{P_{out}}} = \lim_{CR\to 0} \frac{CR}{\sqrt{1 - e^{-CR^2}}} = 1. \tag{4.18}$$

Thus, as the clipping level increases, more part of the signal is retained, the amount of distortion decreases and the SNR increases.

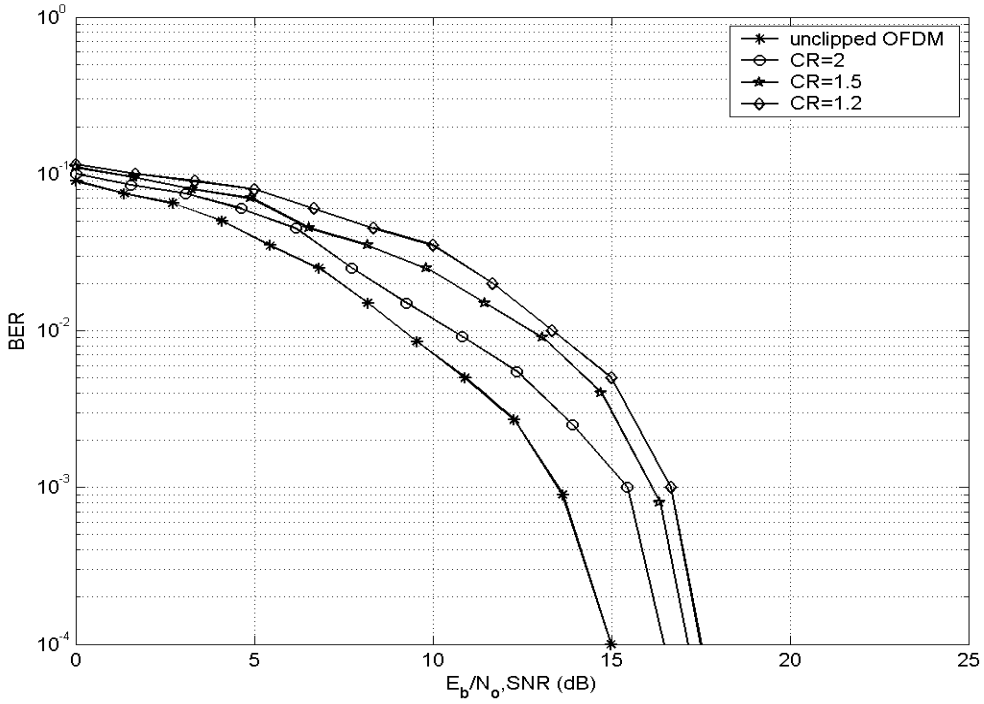

Figure 4.2 BER performance of clipping technique.

We have now plotted the BER in additive white Gaussian noise (AWGN) channel versus the signal-to-noise ratio in dB in Figure 4.2. The BER plot for unclipped OFDM is also shown. We see that clipping causes in-band noise, which causes degradation in the BER performance of OFDM. To achieve a BER of 10^{-2} the unclipped OFDM requires 2 dB less signal-to-noise ratio as compared to clipped OFDM. Also the BER performance was studied for various clipping ratios. As the clipping ratio is increased the BER performance comes closer to that of unclipped OFDM. For hard clipping (CR= 1.2), the degradation is more than 5 dB at the 10^{-2} BER level. In order to understand the reduction in PAPR using the clipping technique we consider the probability that the PAPR λ exceeds a given threshold $\overline{\lambda}$, which is represented by the complementary cumulative distribution of λ;

$$F_{\lambda}^{c}(\overline{\lambda}) = \Pr(\lambda > \overline{\lambda}) = 1 - F_{\lambda}(\overline{\lambda}), \tag{4.19}$$

where, $F_\lambda(\lambda)$ is the cumulative distribution of the PAPR. From [48], [54] the PAPR of the clipped OFDM signal may be bounded as

$$\lambda \le \frac{A_{\max}^2}{P_{out}} = \frac{CR^2}{1-e^{-CR^2}} \tag{4.20}$$

Figure 4.3 depicts the complementary cumulative distribution function (CCDF) of the PAPR of OFDM signal at data rate of X bps. We use the CCDF because the average power is not constant and so an absolute value for PAPR reduction is meaningless to study. The signal utilizes BPSK, QPSK, 16PSK and 64PSK constellations. Clipping has little effect on BPSK OFDM. We see that 2.2 dB reduction is obtained in the PAPR with clipping when compared to unclipped OFDM signal.

Thus, clipping reduces the PAPR but at the expense of distortion and degradation in the BER performance of OFDM. Increased BER due to clipping may be reduced using the forward error correction coding [55]. Another technique would be using phase and amplitude correction which limits the out of band noise and the BER but degrades the PAPR statistics.

4.4 Probabilistic Approach

Another approach to reduce the PAPR is called the probabilistic technique, which doesn't aim at reducing the maximum signal amplitude, but rather the occurrence of the peak values [40]. The basic idea is to manipulate the OFDM signal so that the large values occur with lower probability. The general probabilistic approach is to introduce some redundancy. This resembles block coding, but the goal is not to eliminate the peaks, but only to make them less frequent. The basic way to achieve this is a linear transformation as shown in (4.21) below. In this equation, Y_n are elements of the N-point input vector Y of the IFFT and X_n are the elements of the original domain vector X.

$$Y_n = A_n.X_n + B_n \quad 1 \le n \le M . \tag{4.21}$$

The goal is to find the M point vectors A and B with elements A_n and B_n respectively, such that the transmit symbol y=IFFT(Y) has small probability of peaks. Two techniques,

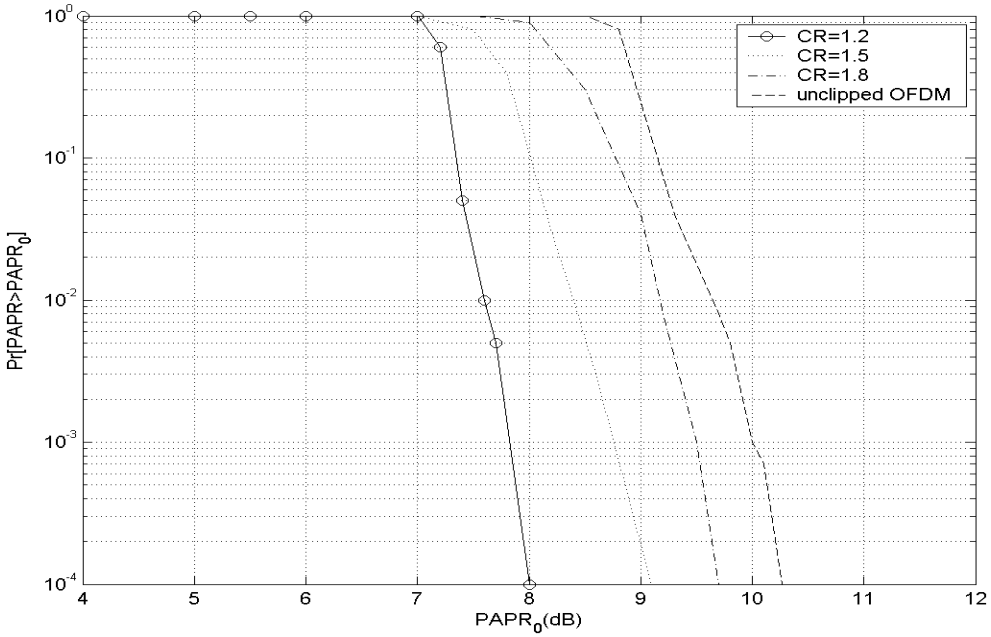

Figure 4.3 CCDF of OFDM using different clipping ratios.

Selected Mapping (SLM) and Partial Transmit Sequences (PTS) [56] have been proposed, they try to select a good A, while B is equal to the zero vector. They both use the restriction that the N components of A all have unit amplitude and it results in a pure rotation vector.

$$A_n = e^{j\theta_n}, \theta_n \in [0, 2\pi], \quad 0 \le n \le M \tag{4.22}$$

Tone Injection (TI) and Tone Rejection (TR) optimize B, while A is set to all one vector. Each of these techniques have different performance versus overhead and complexity trade offs [57].

4.4.1 Selective Mapping Approach

The basic idea is to generate a number D, of statistically independent sequences of data and the sequence with lowest PAPR is selected for transmission. These independent data sequences are generated using M fixed rotation vectors A_m with $1 \le m \le M$ .The first modified vector Y_1 can be chosen as the unchanged original vector X, which means that

A_1 is the all one vector. This approach was first proposed for only one alternative vector i.e. M=2.The figure 4.4 below explains this approach. It involves calculating all M alternative time domain symbols Y_D in parallel and selecting one with the smallest PAPR and that symbol is then transmitted. We will focus our study on the reduction of PAPR using the random phase shifting technique.

4.4.2 Random Phase Shifting

An OFDM signal can be represented as,

$$s(t) = \sum_{m=0}^{M-1} b_m e^{j2\pi(m/T)t}, \tag{4.23}$$

where, b_m is the symbol of the m^{th} subchannel at interval T and N is the number of subcarriers. The power of *s(t)* is given by:

$$p(t) = |s(t)|^2 . \tag{4.24}$$

The variation of the instantaneous power of OFDM signal from the average is given as

$$\Delta P(t) = P(t) - E[P(t)], \tag{4.25}$$

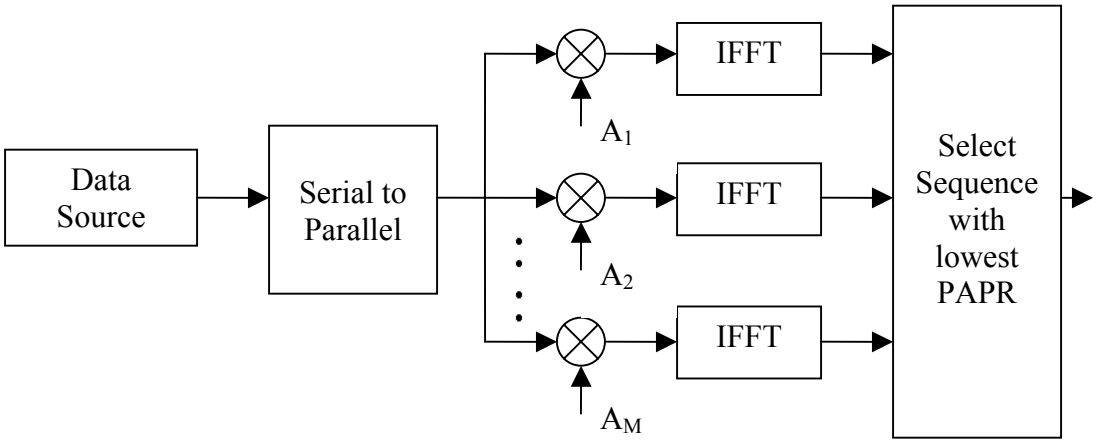

Figure 4.4 Selective Mapping technique to reduce PAPR.

and accordingly, the power variance of OFDM signal, denoted by *PV*, can be written as,

$$PV = \frac{1}{T}\int_0^T (\Delta P(t))^2 \, dt \, . \tag{4.26}$$

As given in [58], the PAPR and the power variance are related by the relationship,

$$Q\left(\frac{PAPR-1}{\sqrt{PV}}\right) + Q\left(\frac{1}{\sqrt{PV}}\right) = \beta \, , \tag{4.27}$$

where, β denotes the probability that *P(t)* be less than or equal to P_{max} and

$$Q(y) = \frac{1}{\sqrt{2\pi}}\int_y^\infty e^{-u^2/2} \, du \, . \tag{4.28}$$

From (4.27) it can be seen that for a fixed β the OFDM signal with high PAPR has a high value of *PV*. Because of less computational burden in calculation of PV, we can easily find the value of PAPR by calculating the power variance. The Figure 4.5 below illustrates the block diagram of OFDM with phasing showing the principle of adding phase shifts to the OFDM symbols. In this technique, after serial to parallel conversion, each bit is modulated onto the carriers, and separability is maintained through use of carefully selected phase offsets [59].

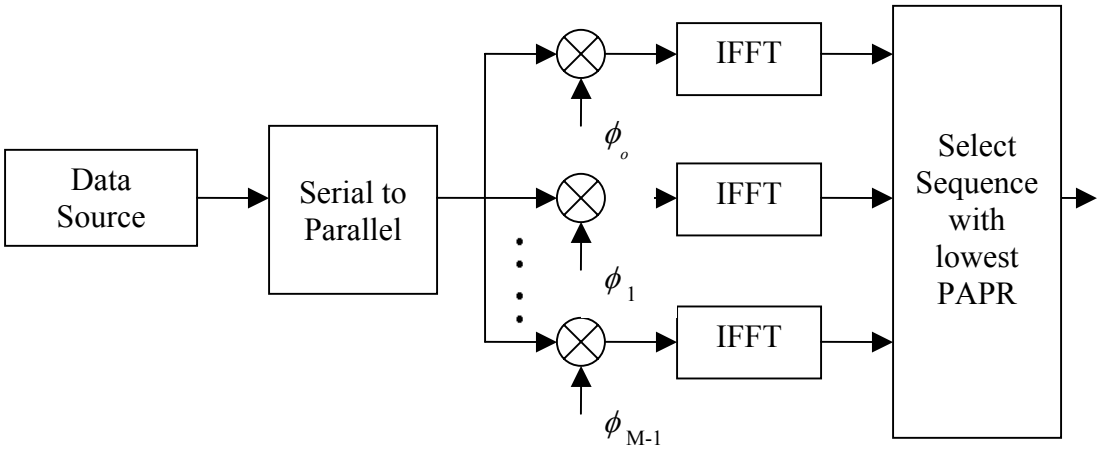

Figure 4.5 Random phase shifting method to reduce PAPR.

The OFDM signal with phase shifting can be written as,

$$s(t) = \sum_{m=0}^{M-1} b_m e^{j2\pi((m/T)t+\phi_m)}, \tag{4.29}$$

where, $2\pi\phi_m$ is the mth subcarrier phase shift. Adding random phases to each subcarrier will change the power variance of OFDM signal. In the random phase updating algorithm, the phase of each subcarrier is updated by a random increment as:

$$(\phi_m)_i = (\phi_m)_{i-1} + (\Delta\phi_m)_i \quad m=0, 1, \ldots, M-1 \tag{4.30}$$

where, *i,* is the iteration index and $(\Delta\phi_m)_i$ is the phase increment of the m^{th} subcarrier at the i^{th} iteration. In random phase updating method, the initial phase, i.e., $(\phi_m)_0$, can be considered zero. Consequently, a random phase increment is generated and phase is updated by adding the increment to the phase of that subcarrier. Flow chart in Figure 4.6 shows this iterative phase updating. This addition of phase offset allows the receiver to separate the bits co-located on identical carriers. From Figure 4.7 we see the BER performance of OFDM with random phase updating compared with OFDM with no phase change. We observe a slight gain in the BER performance of phase updated OFDM when perfect knowledge of the phase changes is available at the receiver. This gain in performance is due to the frequency diversity benefit of phase changed OFDM. Note that this is only possible when the phase changes are completely known by the receiver. Also seen how the BER performance of random phase updating with imperfect knowledge of the added phases is degraded. We observe that even a 10% uncertainty (error) in the phase information at the receiver, (as a result of phase updating algorithm), causes a large degradation to the BER performance of the system. In addition to the improved performance benefit, the phase updating algorithm improves the PAPR as well. From (4.11) we have seen that the PAPR for OFDM is lower bound on the number of subcarriers. From the equation of OFDM using random phase shifting we see that when one bits carriers add coherently, other bit's carriers do not add coherently because when $s_k(t)$ reaches its maximum, $s_j(t)$ (where $j \neq k$), is at a minimum i.e. $P_j << P_k$. Therefore, if

we consider worst case scenario the PAPR of OFDM with random phase shifting is given by,

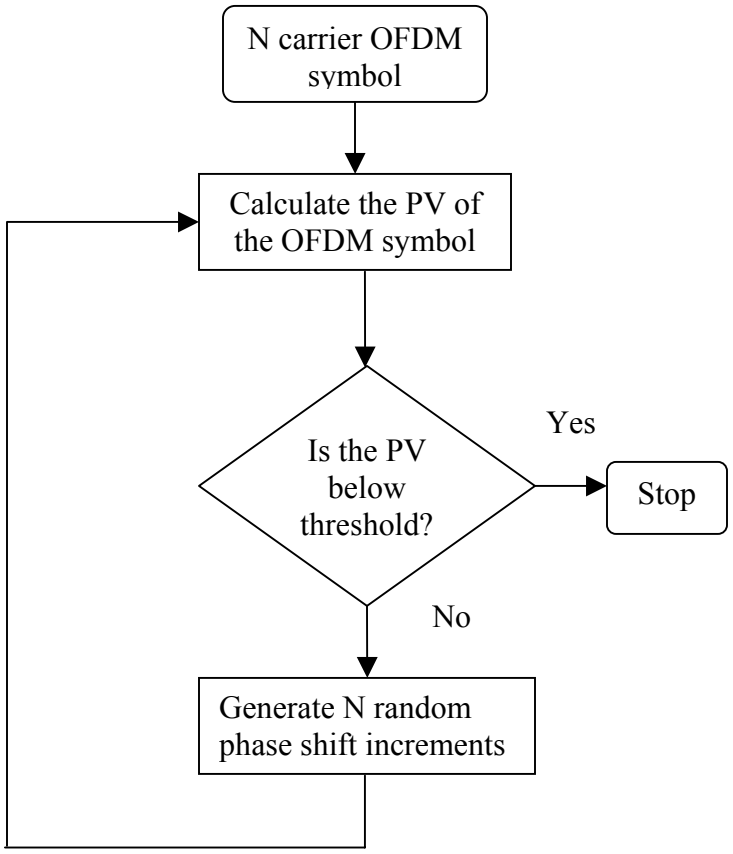

Figure 4.6 Random phase shift algorithm.

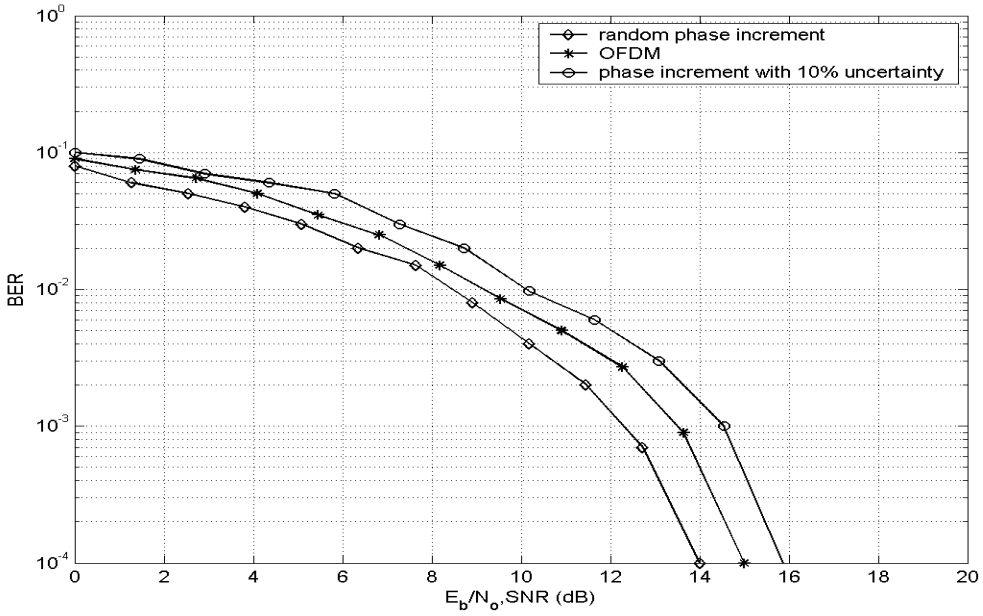

Figure 4.7 BER performance of phase increment technique.

$$PAPR = \frac{\left(\frac{1}{2}\max_{0<t<Ts}|s(t)|\right)^2}{NP} << N. \tag{4.31}$$

Thus we achieve reduction in PAPR while using the random phase increment algorithm. We later tried a more tedious algorithm than the one mentioned above. It is a modification of the above algorithm but instead of stopping when the PAPR was found to be lesser than the threshold, we repeated the algorithm a few more number of times. The reduced power variance is now set as the new threshold and the phases are incremented and the new power variance is compared with the reduced power variance which was set as the threshold before. This is repeated for a few iterations till there is no further significant reduction in the phase shift or till the defined number of iterations. This algorithm is shown in Figure 4.8. In order to compare the performance of the PAPR reduction algorithm we plot the complementary cumulative density function (CCDF), i.e.

the probability that the OFDM symbol will exceed a particular PAPR value ($PAPR_o$). Figure 4.9 compares the achieved reduction in PAPR using the phase updating method.

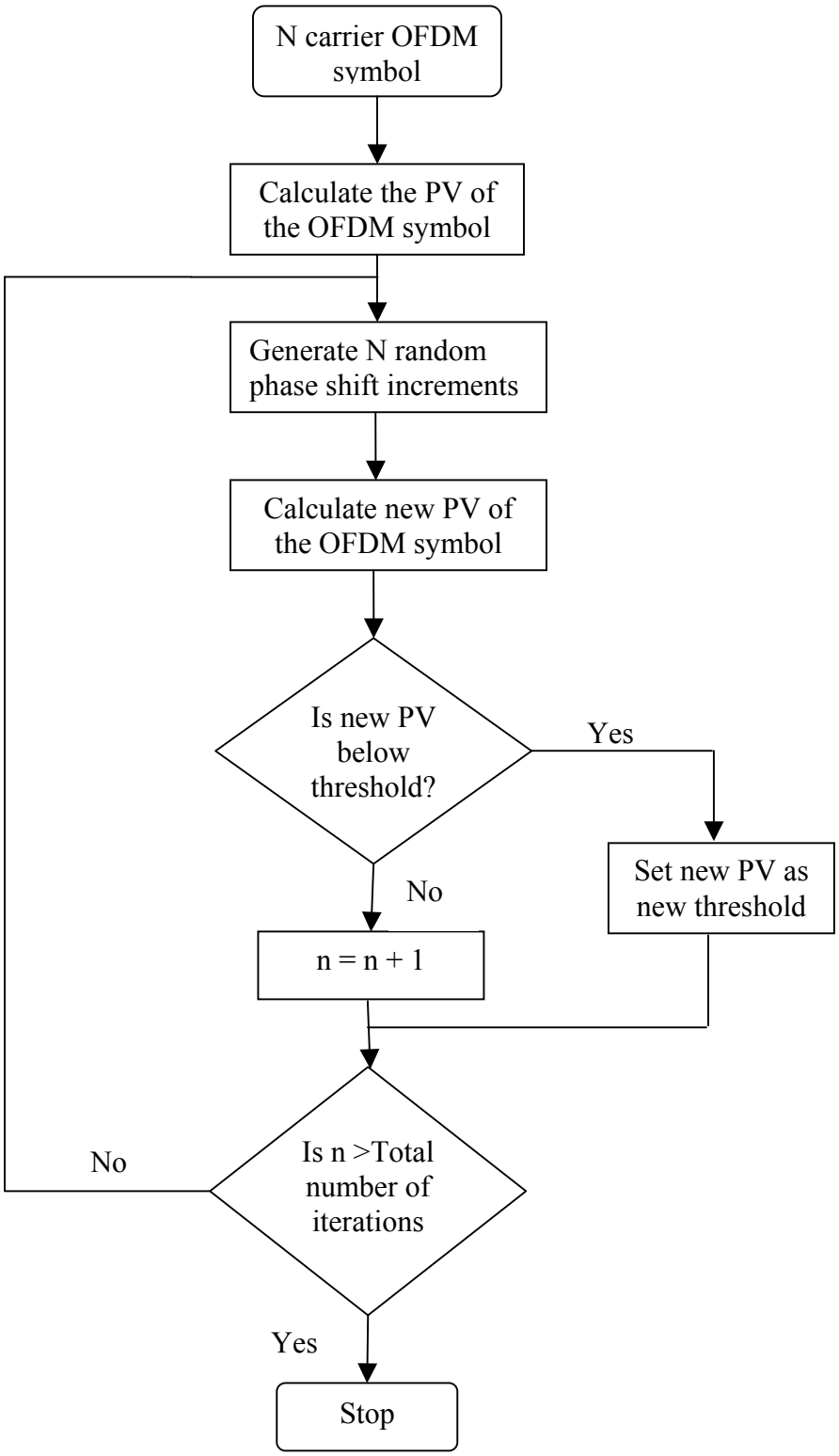

Figure 4.8 Phase increment algorithm with large number of iterations.

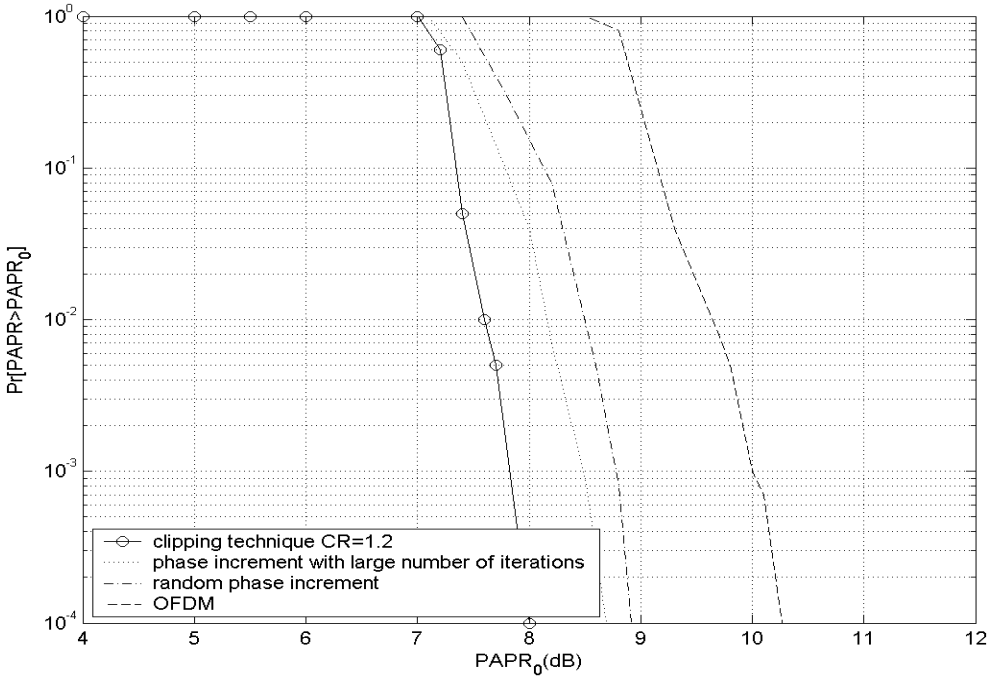

Figure 4.9 CCDF of OFDM using clipping and phase increment technique.

As shown the random phase incrementing algorithm is effective in reducing the PAPR of OFDM. We have used a uniform distribution for the distribution of phase increments. ($\Delta\phi_m = Unif[o, x]$), where $x \in \{0.1, 0.25, 0.5, 0.75, 1\}$. We have plotted the CCDF function of clipping technique when CR=1.2 alongside and observe that the clipping technique gives a lower PAPR compared to the random phase increment algorithm but the BER performance for the same clipping ratio is degraded when compared with the phase incrementing algorithm. We also see that as the number of iterations is increased and we keep changing the thresholds until no further reduction is possible, we get a lower PAPR compared to the random phase increment with fixed threshold technique. It is quite clear that when the standard deviation of phase increments is small, large number of iterations is required to cause significant reduction in the PAPR.

When we increase the variance of the phase shift increments, the number of iterations required to reach the threshold is less.

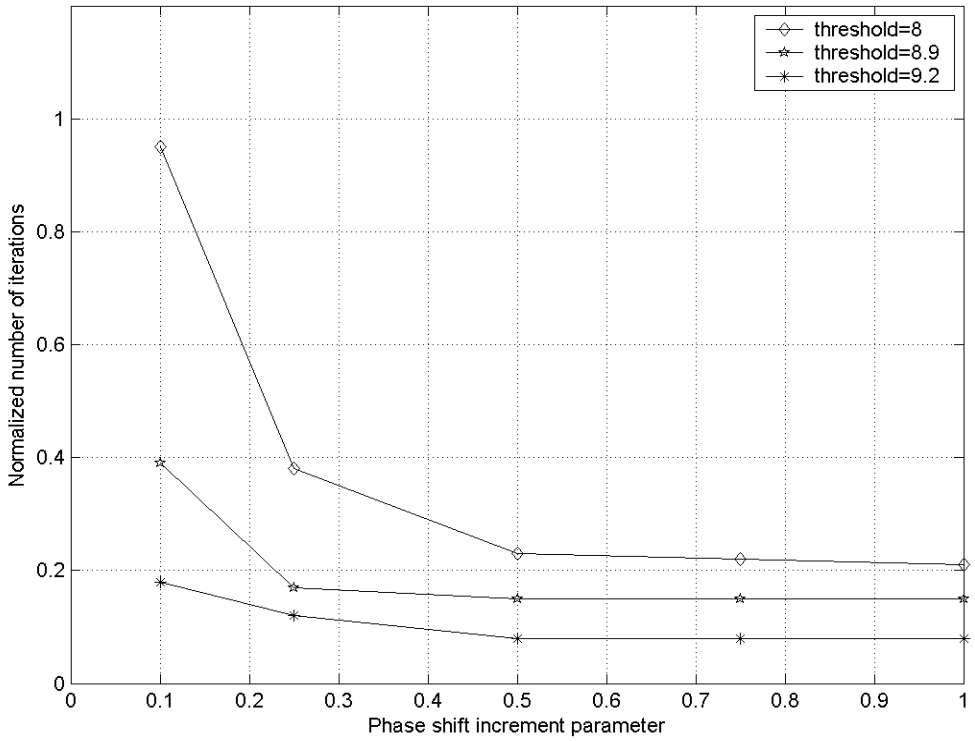

Figure 4.10 Relation between the number of iterations and the phase shift increment parameter.

Since lower threshold or smaller power variance needs more number of iterations to select the proper phases for the subcarriers. This is shown in Figure 4.10. Also, the threshold level has a significant effect on the number of iterations. Efficient reduction in PAPR is obtained when the correct initial threshold is selected. The main drawback of this algorithm is the high complexity and the side information required. When the number of carriers increases this method becomes computationally very difficult as the number of power variance calculation increases. Besides, because of the large number of phases involved with the large number of carriers leads to a large amount of side information to be transmitted. These phase increments have to be known at the receiver. To lessen the problem, Partial Transmit Sequences algorithm was suggested. This involves

quantization and grouping of the random phase increments. Quantization of the phase shifts i.e. 2 for BPSK, 4 for QPSK and so on, decreases the number of bits necessary to represent each phase shift which leads to a reduced complexity of the algorithm. Grouping implies that all subcarriers put in one group get the same phase shift increment. Using a combination of these two methods the complexity is reduced. As mentioned other probabilistic approaches include, Tone Reduction and Tone Injection. Each technique has its own implementation complexity which is one of the major factors to prefer one technique over the other. New techniques are being worked upon, [60] , [61] to reduce implementation complexity and to achieve better performance.

Out of the clipping and probabilistic approach discussed here, to reduce the PAPR of OFDM, it is seen that the clipping technique suffers from degraded BER performance but the technique is simpler and gives a reduced PAPR. Using the probabilistic approach we get a comparatively reduced PAPR and the BER performance is better too, but it suffers because of the number of iterations and hence due to the complexity. Adaptively loading the bits on the subcarriers followed by the PAPR reduction technique makes way for efficient transmission of data through the channel and gives a better spectral efficiency than the current OFDM technique used.

CHAPTER 5
CONCLUSIONS AND FUTURE WORK

5.1 Conclusion and Contributions

This thesis presents an in-depth study of the bit loading techniques and the peak to average power reduction methods for Adaptive OFDM. In the beginning of this thesis we have reviewed the fundamentals of OFDM and the bandwidth efficient advantage it offers against single carrier systems. OFDM can easily be implemented using IFFT and FFT algorithm. By inserting guard time that is longer than the delay spread of the channel, an OFDM system is able to mitigate intersymbol interference (ISI). In AWGN, OFDM has the same performance as a single carrier coherent transmission scheme but due to its lower symbol rate robustness against frequency selective fading and ISI is achieved.

We have discussed the effective control on the BER of the transmission and the increased spectral efficiency is achieved using Adaptive OFDM, and it also significantly reduces the need for forward error correction. Accurate channel state information is required by the transmitter to suitably load the bits onto the subcarriers. Imperfect channel state information arising from the noise at the receiver as well as because of the outdated information from the time varying channel reaching the transmitter can be dealt with by considering the estimation of the channel and then adapting the transmission parameters. The noisy estimation at the receiver does not hinder the performance of adaptive OFDM but the impact of channel mismatch in the presence of quickly varying channel is significant and increases as the delay in the channel estimation increases.

Investigation is done on the loading of the bits on the subcarriers by optimally varying one of the parameters among the data rate, instantaneous BER and the total transmit power. The choice of the bit loading technique is application specific. Rate adaptive technique offers maximum spectral efficiency and is thus used for high speed data transmission where maximum spectral efficiency is desired at fixed BER. The fixed

threshold rate adaptive algorithm overcame the quantization and the complexity issue occurring with the Chow rate adaptive algorithm. For secured voice transmission, error rate has to be minimized and so fixed throughput technique is used. On similar lines to the SNR comparison approach used in the rate adaptive fixed threshold technique we have proposed the blockwise loading fixed throughput algorithm. This technique is less complex to implement compared to the cost algorithm. Using the blockwise loading algorithm we studied the BER performance for different data rate and observed that as the data rate increases the BER performance decreases. The BER performance of the power adaptive technique was compared with that of the rate adaptive technique and we observed that the two techniques met the BER constraints well but the performance of the power adaptive technique was better since the rate adaptive technique in an attempt to maximize the bit rate uses higher order modulation levels and so a higher error rate. Whereas the power adaptive technique uses fixed data rate and so at large SNR it has control on the number of bits loaded and hence on the number of erroneous bits and so a better BER.

The clipping and probabilistic approach to reduce the peak to average ratio of OFDM were presented. Clipping technique is simpler to implement but gives a low BER performance. It was seen that the phase shifting technique gives a slight gain in the BER performance when compared with OFDM with no phase change. In addition to this improved performance benefit, the phase updating algorithm reduces the PAPR as well. A modification of this random phase shifting algorithm is proposed. Instead of stopping when the PAPR was found to be less than the threshold, the reduced power variance is set as the new threshold and we repeat the algorithm for a fixed number of iterations or until there is no further significant drop in PAPR. This technique is more complex to implement than the conventional approach but it is seen that it gives a reduced PAPR compared to the phase increment with fixed threshold technique.

5.2 Future Work

In this research coding techniques was not considered and in the future we can use the bit loading technique combined with coding technique. We can also extend this work

for time division duplex channels when there is no dedicated feedback path between the transmitter and the receiver. In order to achieve greater efficiency we can experiment with alternating the use of rate and fixed throughput technique on fading channels. In case of bad channel conditions we can allocate the transmit power to send data at fixed rate and when the channel conditions improve we can reallocate the power to maximize the data rate. Thus we could then support the simultaneous requirements for high data rate (data communications) and fixed data rate (voice) on fading channels. We have also assumed no carrier frequency offset between the transmitter and the receiver and also perfect symbol timing at the receiver. In the future, we can examine the performance of the adaptive algorithms under the frequency offset, phase noise, and symbol timing error conditions. We need to devise ways to improve the BER performance in case of imperfect channel state information in case of fast varying channels in outdoor environment. Adaptively loading the bits on the subcarriers followed by the PAPR reduction technique could make way for efficient transmission of data through the channel and finally a complete adaptive OFDM system with better spectral efficiency and BER performance to replace the current system used in the wireless standards.

REFERENCES

REFERENCES

[1] D. Matiae, "OFDM as a possible modulation technique for multimedia applications in the range of mm waves," *Introduction to OFDM*, II edition, TUD-TVS, Oct. 1998.

[2] L. J. Cimini, Jr., "Analysis and simulation of a digital mobile channel using orthogonal frequency division multiplexing," *IEEE Transactions on Communications*, vol. 7, pp. 665-675, July 1985.

[3] Richard Van Nee, Ramjee Prasad, *OFDM for Wireless Multimedia Communications*, Boston-London, Artech House, 2000.

[4] E. Lawrey, *Adaptive techniques for multiuser OFDM*, Thesis for PhD, James Cook University, Dec. 2001.

[5] B. Sueur, D. Castelain, G. Degoulet, M. Riviere and B. LeFloch, "Digital terrestrial broadcasting of audiovisual signals," *Spectrum 20/20 conference*, Toronto, Sept. 1992.

[6] B.-L. P. Cheung, *Simulation of Adaptive Array Algorithms for OFDM and Adaptive Vector OFDM Systems*, Thesis for PhD, Virginia Polytechnic Institute and State University, Sept. 2002.

[7] Ioannis Zaptis, *Performance analysis of the OFDM technique in fading environments*, Project Report for MS degree, The University of Tennessee, Spring 2001

[8] Theodore S. Rappaport, *Wireless Communications: Principles and Practice*, New Jersey: Prentice Hall, 1996.

[9] R. Steele and W. Webb, "Variable rate QAM for data transmission over Rayleigh fading channels," *Proceedings of Wireless*. Calgary, Alta., Canada, pp. 1-14, 1991.

[10] H. A. Qureshi, *Performance improvement of adaptive OFDM system in the presence of imperfect channel state information*, Thesis for MS degree, The University of Tennessee, May 2003.

[11] Q. Su and S. C. Schwartz, "Effects of Imperfect channel information on adaptive loading gain of OFDM," *Proceedings of the Vehicular Technology Conference*, pp. 1397-1404, Fall 2000.

[12] M. Sandell and O. Edfors, "A comparative study of pilot-based channel estimators for wireless OFDM," *Research Report TULEA 1996:19*, Division of the Signal Processing, Lulea University of Technology, Sep. 1996.

[13] V. D. Beek, J. J., O. Edfors, M. Sandell, S. K. Wilson and P. O. Borjesson, "On channel estimation in OFDM systems," *Proceedings of the 45th IEEE Vehicular Technology Conference*, Rosemont, IL, pp. 715-719, July 1995.

[14] M. R. Souryal and R. L. Pickholtz, "Adaptive modulation with imperfect channel information in OFDM," *IEEE International Conference on Communications*, vol. 6, pp. 1861-1865, June 2001.

[15] E. Lawrey, "Multiuser OFDM," *5th International Symposium on Signal Processing and its Applications*, Brisbane, Australia, pp. 761-764, Aug. 1999.

[16] J. G. Proakis, *Digital Communications*, 3rd ed. New York: McGraw-Hill, 1995.

[17] S. Ye, R. S. Blum and L. J. Cimini, Jr., "Adaptive modulation for variable-rate OFDM systems with imperfect channel information," *Proceedings of the IEEE Vehicular Technology Conference*, pp. 767-772, Spring 2002.

[18] A. Leke and J. M. Cioffi, "Multicarrier systems with imperfect channel knowledge," *Proceedings PIMRC*, pp. 549-553, 1998.

[19] Y. Li, L. J. Cimini, Jr. and N. R. Sollenberger, "Robust channel estimation for OFDM systems with rapid dispersive fading channels," *IEEE Transactions on Communications*, vol. 46, pp. 902-915, July 1998.

[20] Q. Su, L. J. Cimini Jr. and R S. Blum, "On the problem of channel mismatch in constant-bit-rate adaptive modulation for OFDM," *Proceedings of the 55th IEEE Vehicular Technology Conference*, vol.2, pp. 585-589, May 2002.

[21] S. G. Chua and A. Goldsmith, “Variable-rate variable-power MQAM for fading channels,” *Proceedings of the 46th IEEE Vehicular Technology Conference*, pp. 815-819, 1996.

[22] A. Goldsmith, “Adaptive modulation and coding for fading channels,” *Proceedings of the IEEE Information Theory and Communications Workshop*, pp. 24-26, June 1999.

[23] S. T. Chung and A. J. Goldsmith, “Degrees of freedom in adaptive modulation: a unified view,” *IEEE Transactions on Communications*, vol. 49, pp. 1561-1571, Sep. 2001.

[24] P. S. Chow, J. M. Cioffi and J. A. C. Bingham, “A practical discrete multitone transceiver loading algorithm for data transmission over spectrally shaped channels,” *IEEE Transactions on Communications*, vol. 43, pp. 773-775, Feb.-March 1995.

[25] J. Jang, K. B. Lee, and Y.-H. Lee, "Transmit Power and Bit Allocations for OFDM Systems in a Fading Channel," *Proceedings of the IEEE Global Communications Conference*, pp. 858-862, December 2003.

[26] H. S. Chu, C. K. Ann, “Bit and subcarrier allocation for OFDM transmission using adaptive modulation,” *Proceedings of the 7th Korea-Russia International Symposium*, pp. 82-85, 2003.

[27] T. Keller and L. Hanzo, “Adaptive multicarrier modulation: A convenient framework for time-frequency processing in wireless communications,” *Proceedings of the IEEE*, vol. 88, no. 5, pp. 611-640, May 2000.

[28] T. Keller and L. Hanzo, “Adaptive modulation techniques for duplex OFDM transmission,” *Proceedings of the IEEE Vehicular Technology Conference*, vol. 49, pp. 1893-1902, 1999.

[29] A. T. Toyserkani, J. Ayan, S. Naik, “Subcarrier based adaptive modulation in HIPERLAN/2 system,” *Radio communication Systems*, KTH Royal Institute of Technology, Sweden, Fall 2003.

[30] C.-J. Ahn and I. Sasase, “The effects of modulation combination, target BER, Doppler frequency, and adaptation interval on the performance of adaptive

OFDM in broadband mobile channel," *IEEE Transactions on Consumer Electronics*, vol. 48, Issue 1, pp. 167-174, Feb.2002

[31] R. F. H. Fisher and J. B. Huber, "A new loading algorithm for discrete multitone transmission," *Proceedings of the IEEE Global Telecommunications Conference*, pp. 724-728, 1996.

[32] D. Hughes-Hartogs, *Ensemble modem structure for imperfect transmission media*, U.S. Patents Nos. 4679227, July 1987; 4731816, March 1988 and 4833706, May 1989.

[33] M. Minto, D. Ragazzi, L.Agarossi and L. Giangaspero, "Minimum transmission power algorithm for OFDM based flexible systems," *Workshop on Broadband Wireless Ad-Hoc Networks and Services*, France, September 2002.

[34] P. Bansal, and A. Brzezinski, *Adaptive Loading in MIMO/OFDM systems*, Project Report, Stanford University, December 2001.

[35] S. T. Chung and A. Goldsmith, "Adaptive multicarrier modulation for wireless systems," *Conference Record of the Thirty-Fourth Asilomar Conference on Signals, Systems and Computers*, vol. 2, pp. 1603-1607, Oct-Nov 2000.

[36] H. Matsuoka, S. Sampei, N. Morinaga and Y. Kamio, "Adaptive modulation system with variable coding rate concatenated code for high multi-media communications systems," *Proceedings of the 46th IEEE Vehicular Technology Conference*, pp. 478-491, 1996.

[37] V. K. N. Lau and M. D. Macleod, "Variable rate adaptive trellis coded QAM for high bandwidth efficiency applications in Rayleigh fading channels," in *Proceedings of the IEEE Vehicular Technology Conference*, pp. 348-352, 1998.

[38] A. D. Valkanas, P. I. Dallas, G. J. Karachalios and A. D. Poularikas, "Adaptivity on an OFDM fixed wireless access system," *Proceedings of the 34th Southeastern Symposium on System Theory*, pp. 458 – 462, March 2002.

[39] K. J.Hole, G. E. Øien, and H. Holm, "Adaptive coded modulation for wireless OFDM channels: Upper bounds on average spectral efficiency and influence of imperfect channel knowledge," *Proceedings of the IEE Conference Getting the Most out of the Radio Spectrum*, London, UK, Oct. 2002.

[40] C. Schurgers, M. B. Srivastava, *A systematic approach to peak to average power ratio in OFDM*, Project Report, Electrical Engineering Department, University of California at Los Angeles (UCLA), Spring 2003.

[41] S. B. Slimane, "Peak to average power ratio reduction of OFDM signals using pulse shaping," *IEEE Global Telecommunications Conference*, vol. 3, pp 1412 – 1416, November-December 2000.

[42] S. B. Slimane, "Peak to average power ratio reduction of OFDM signals using broadband pulse shaping," *IEEE Proceedings of the 56th Vehicular Technology Conference*, vol. 2, pp.889 – 893, Sept. 2002.

[43] N. Carson and T. A. Gulliver, "PAPR reduction of OFDM using selected mapping, modified RA codes and clipping," *Proceedings of the 56th IEEE Vehicular Technology Conference*, vol.2, pp.1070 – 1073, Sept. 2002.

[44] A. E. Jones, T. A. Wilkinson and S.K. Barton, "Block coding scheme for reduction of peak to mean envelope power ratio of multicarrier transmission schemes," Electronic Letters, vol.30, p. 2098-2099, 1994.

[45] Charles J. Meyer, "Measuring the peak to average power of digitally modulated signal," *Boonton Electronics*, Application Note AN-50, pp. 1-5, April 1993.

[46] A. D. S. Jayalath and C. Tellambura, "Reducing the peak-to-average power ratio of orthogonal frequency division multiplexing signal through bit or symbol interleaving," *IEEE Electronic Letters*, vol. 36, pp. 1161 –1163, June 2000.

[47] Ali Behravan and Thomas Eriksson, "PAPR and other measures for OFDM systems with nonlinearity," *Proceedings of the 5th International Symposium on Wireless Personal Multimedia Communications*, Oct. 2002.

[48] H. Ochiai and H. Imai, "Performance of the deliberate clipping with adaptive symbol selection for strictly band limited OFDM systems," *IEEE Journal on Selected Areas in Communications*, vol. 18, no. 11, pp. 2270-2277, November 2000.

[49] T. A. Wilkinson and A.E. Jones, "Minimization of the peak to mean envelope power ratio in multicarrier transmission schemes by block coding," *Proceedings of the Vehicular Technology Conference*, pp. 825-831, July 1995.

[50] M. Friese, “Multicarrier modulation with low peak to average power ratio,” *IEEE Electronics Letters*, vol. 32, Issue 8, pp. 713 – 714, April 1996.

[51] Xiadong Li and L.J. Cimini Jr., “Effects of clipping and filtering on the performance of OFDM,” *IEEE Communications Letters*, vol. 2, Issue 5 , pp. 131-133, May1998

[52] J. Armstrong, "Peak to average power reduction in digital television transmitters", *DICTA conference*, Melbourne, pp.19-24, January 2002.

[53] J. Armstrong, “New OFDM peak to average power reduction scheme,” *Proceedings of the 53rd IEEE Vehicular Technology Conference*, vol. 1, pp. 756 – 760, May 2001.

[54] H. Ochia and H. Imai, “On the distribution of the peak to average power ratio in OFDM signals,” *IEEE Transactions on Communications*, vol. 49, Issue 2, pp. 282 – 289, February 2001.

[55] D. Wulich and L. Goldfeld, “Reduction of peak factor in orthogonal multicarrier modulation by amplitude limiting and coding,” *IEEE Transaction on Communications*, vol. 47, pp. 18-21, Jan 1999.

[56] L. J. Cimini and N. R. Sollenberger, “Peak to average power ratio reduction of an OFDM signal using partial transmit sequences,” *IEEE Communications Letters*, vol.4, no. 3, pp. 86-88, March 2000.

[57] S. Müller, J. Huber, “A comparison of peak power reduction schemes for OFDM,” *Proceedings of the Global Telecommunications Conference*, pp. 1-5, November 1997

[58] H. Nikookar and K. S. Lidsheim, “Random phase updating algorithm for OFDM transmission with low PAPR,” *IEEE Transactions on Broadcasting*, vol. 48, no.2. pp. 123-128, June 2002.

[59] D. A. Wiegandt, Carl R. Nassar and Z. Wu, “Overcoming PAPR issues in OFDM via carrier interferometry codes,” *Proceedings of the IEEE Vehicular Technology Conference*, Atlantic City, NJ, pp. 660-663, Oct. 2001.

[60] Ermolova, Natalia, "New companding transform for reduction of peak-to average power ration," *Proceedings of the IEEE Vehicular Technology Conference*, Vancouver, Canada, vol. 3, pp. 1404- 1407, 24-28 Sept. 2002.

[61] A.D.S Jayalath, C. Tellambura, "A blind SLM receiver for PAR-reduced OFDM", *Proceedings of the 56th IEEE Vehicular Technology Conference*, vol.1, pp. 219 – 222, Sept. 2002.

VITA

Jaideep Rajan Shahri was born in Mumbai, India on April 9, 1980. He was raised in the same place and went to grade school at Arya Vidya Mandir and high school at D.G. Ruparel College. He graduated with a B.E in Electronics Engineering from Thadomal Shahani Engineering College in 2002. From there, he went to University of Tennessee, Knoxville and received his M.S. in Electrical Engineering in 2004. During his stay there, he worked as a Graduate Assistant at the Innovative Technology Center and also did research for Wireless Communication Research Group.